AD-785 247

A LIFTING-SURFACE PROGRAM FOR TRAPEZOIDAL CONTROL SURFACES WITH FLAPS

Justin E. Kerwin, et al

Massachusetts Institute of Technology

Prepared for:

Office of Naval Research

August 1974

DISTRIBUTED BY:

NTIS

National Technical Information Service
U. S. DEPARTMENT OF COMMERCE
5285 Port Royal Road, Springfield Va. 22151

SECURITY CLASSIFICATION OF THIS PAGE (When Data Entered)

REPORT DOCUMENTATION PAGE		READ INSTRUCTIONS BEFORE COMPLETING FORM
1. REPORT NUMBER 74-15	2. GOVT ACCESSION NO.	3. RECIPIENT'S CATALOG NUMBER AD 785 247
4. TITLE (and Subtitle) A LIFTING-SURFACE PROGRAM FOR TRAPEZOIDAL CONTROL SURFACES WITH FLAPS		5. TYPE OF REPORT & PERIOD COVERED Final Report
		6. PERFORMING ORG. REPORT NUMBER
7. AUTHOR(s) Justin E. Kerwin, Bohdan W. Oppenheim		8. CONTRACT OR GRANT NUMBER(s) N00014-67-A-0204-0067
9. PERFORMING ORGANIZATION NAME AND ADDRESS Dept. of Ocean Engineering, M.I.T., Cambridge, MA 02139		10. PROGRAM ELEMENT, PROJECT, TASK AREA & WORK UNIT NUMBERS
11. CONTROLLING OFFICE NAME AND ADDRESS Office of Naval Research		12. REPORT DATE August, 1974
		13. NUMBER OF PAGES 67
14. MONITORING AGENCY NAME & ADDRESS (if different from Controlling Office)		15. SECURITY CLASS. (of this report) Unclassified
		15a. DECLASSIFICATION/DOWNGRADING SCHEDULE

16. DISTRIBUTION STATEMENT (of this Report)

Distribution of this document is unlimited

17. DISTRIBUTION STATEMENT (of the abstract entered in Block 20, if different from Report)

18. SUPPLEMENTARY NOTES

19. KEY WORDS (Continue on reverse side if necessary and identify by block number)

Control Surfaces
Lifting Surface Theory
Rudders
Ship Maneuvering

20. ABSTRACT (Continue on reverse side if necessary and identify by block number)

A numerical lifting surface procedure is developed specifically for flapped control surfaces with trapezoidal planforms. The procedure uses a discrete vortex approximation with spanwise vortex lines located at constant percentages of the chord. Use of the procedure in obtaining an optimum flapped rudder design is demonstrated. A listing and user's description of the computer program is included.

DD FORM 1 JAN 73 1473 EDITION OF 1 NOV 65 IS OBSOLETE
S/N 0102-014-6601

SECURITY CLASSIFICATION OF THIS PAGE (When Data Entered)

MASSACHUSETTS INSTITUTE OF TECHNOLOGY
Department of Ocean Engineering
Cambridge, MA 02139

Report No. 74-15

A LIFTING-SURFACE PROGRAM FOR TRAPEZOIDAL CONTROL SURFACES WITH FLAPS

by

Justin E. Kerwin
and
Bohdan W. Oppenheim

August 1974

This work was supported by the Office of Naval Research,
Contract N00014-67-A-0204-0067, NR 062-467, MIT OSP 80464.

ia

CONTENTS

		Page
	Abstract	
	Nomenclature	
1.	Introduction	1
2.	Discrete Vortex Arrangement	4
3.	Continuous and Discrete Circulation Distribution	10
4.	Computation of Induced Velocities	18
5.	Computation of Forces	24
6.	Test of Program Accuracy	28
7.	Design Application	33
8.	References	37
	Appendices	
1.	Instruction for Preparing Computer Program Input Data	40
2.	Sample Output	42
3.	Computer Program Listing and Particulars	46
4.	Positioning of Control Points Within Their Own Elements	59
	Figures	
1.	Coordinate System and Notation for Planform Geometry	2
2.	Illustration of a Typical Horseshoe Vortex Element	6
3.	Complete Lattice Arrangement	7
4.	Chordwise and Spanwise Mode Shapes	12
5.	Spanwise Lift Distribution Obtained by Present Program Superimposed on Fig. 13 of [5]	30
6.	Spanwise Distribution of Lift Due to Angle of Attack and Flap Deflection for Rudder Designs of Table 6	36
7.	The Element Used for Estimation of the Error Caused by Control Point Position Deviations	60
	Tables	
1.	Relative Vortex Strength for Eight Chordwise Intervals	15
2.	Relative Vortex Strength for Fifty Chordwise Intervals	16
3.	Variations of Parameters With Extreme Precision Numbers	28
4.	Indentification of Symbols in Fig. 5	31
5.	Effect of Sweep and Taper on Flapped Rudder Characteristics	34

ABSTRACT

A numerical lifting surface procedure is developed specifically for flapped control surfaces with trapezoidal planforms. The procedure uses a discrete vortex approximation with spanwise vortex lines located at constant percentages of the chord. Use of the procedure in obtaining an optimum flapped rudder design is demonstrated. A listing and user's description of the computer program is included.

NOMENCLATURE

(In the order of appearance in the text)

a	effective aspect ratio $\frac{(2s)^2}{A}$
s	semi-span
A	rudder area
f	flap area ratio A_F/A
A_f	flap area
λ	taper ratio c_T/c_R
c_T	tip chord
c_R	root chord
Λ	sweep angle of 1/4 chord
x	chordwise coordinate axis
z	spanwise coordinate axis
$x_L(z)$	leading edge chordwise coordinate
$x_T(z)$	trailing edge chordwise coordinate
i	spanwise panel index of the lattice
j	chordwise panel index of the lattice
m	spanwise index of control points
n	chordwise index of control points
x_{FR}	flap chord at the rudder root
x_{FT}	flap chord at the rudder tip
x_{SR}	skeg chord at the rudder root
x_{ST}	skeg chord at the rudder tip
I_V	spanwise precision number
I_H	chordwise precision number
I	number of chordwise panels on rudder
J	number of spanwise panels on rudder
NF	number of spanwise panels on flap
NS	number of spanwise panels on skeg
$G(x,z)$	nondimensional circulation distribution
α	rudder angle of attack
δ	flap deflection relative to skeg

NOMENCLATURE
(cont.)

$\gamma(x,s)$	dimensional circulation distribution
U	velocity at infinity
$c_{k\ell}$	mode amplitudes
k	spanwise mode index
ℓ	chordwise mode index
K	number of spanwise modes
L	number of chordwise modes
$f_k(\tilde{z})$	kth spanwise mode
$p_\ell(\tilde{s})$	ℓth chordwise mode
$\tilde{z}$	transformed spanwise coordinate
$\tilde{s}$	transformed chordwise coordinate on rudder
$c(z)$	rudder local chord
$\tilde{t}$	transformed chordwise coordinate on flap
P_ℓ	integral of ℓth chordwise mode
$\Gamma(z)$	spanwise circulation distribution
ξ,ζ	coordinates of a general point on a vortex
$v^{(s)}$	velocity induced by spanwise vortex
$v^{(t)}$	velocity induced by trailing vortex
$v_{m,n,i,j}$	velocity induced by the (i,j)th element at the (m,n)th control points
$v_{m,n,k,l}$	velocity induced at the (m,n)th control point by the (k,l)th mode of unit amplitude
$V_{m,n}$	velocity at the (m,n)th control point
ρ	mass density
$C_{L\alpha}(z)$	local lift coefficient per unit angle of attack
$C_{L\delta}(z)$	local lift coefficient per unit flap deflection angle
$C_{L\alpha}$	overall lift coefficient per unit angle of attack
$C_{L\delta}$	overall lift coefficient per unit flap deflection angle
C_{Di}	induced drag coefficient
η	lifting surface efficiency
M_ℓ	first moment of the ℓth chordwise mode function
$\dfrac{x_H(z)}{c(z)}$	local distance of the center of pressure as a fraction of the local chord from the hinge line

NOMENCLATURE
(cont.)

$\frac{x_{LE}(z)}{c(z)}$	local distance of the center of pressure as a fraction of the local chord from the leading edge
$\frac{\bar{x}_H}{\bar{c}}$	resultant chordwise position of the center of pressure relative to the flap hinge line as a fraction of the mean chord
$\bar{c}$	mean chord = $(x_{FR} + x_{FT} + x_{SR} + x_{ST})/2$
C_{DV}	viscous drag coefficient
$\tilde{s}_H$	transformed chordwise coordinate evaluated at the position of the flap hinge

1. INTRODUCTION

This study arose from the need to develop a rational basis for the selection of optimum geometric characteristics for rudders with relatively small flaps. In this case, very minor changes in sweep or taper can effect a major change in the spanwise distribution of flap chord. This, in turn, could be expected to influence the spanwise and chordwise distribution of lift when the flap is deflected. To optimize rudder performance one would like to have a distribution of lift which results in the maximum lift/drag ratio, highest possible stall angle, and minimum control moment for both skeg and flap. Consequently, it is necessary to have the means for estimating spanwise and chordwise distribution of lift for a given geometry.

Ship rudder effective aspect ratios typically fall in the region where neither high aspect ratio nor low aspect ratio theories are valid. One must, therefore, resort to numerical lifting-surface theory to obtain meaningful results.

It seemed most expedient for this application to write a specialized computer program designed to accommodate only trapezoidal planforms of the form shown in Fig. 1. The flap hinge is required to be at right angles to the root section, and the tip chord is required to be parallel to the flow. No restriction is placed on aspect ratio, sweep or taper, provided that the flap hinge emerges from the tip, rather than the leading or trailing edge.

A trapezoidal planform makes a discrete vortex lifting-surface model relatively simple. Unlike the original work of Faulkner [1], or current schemes for propellers [2], the present work employs spanwise vortex lines located at constant percentages of the flap and skeg chord, rather than at right angles to the oncoming flow. This eliminates the problem of vortex

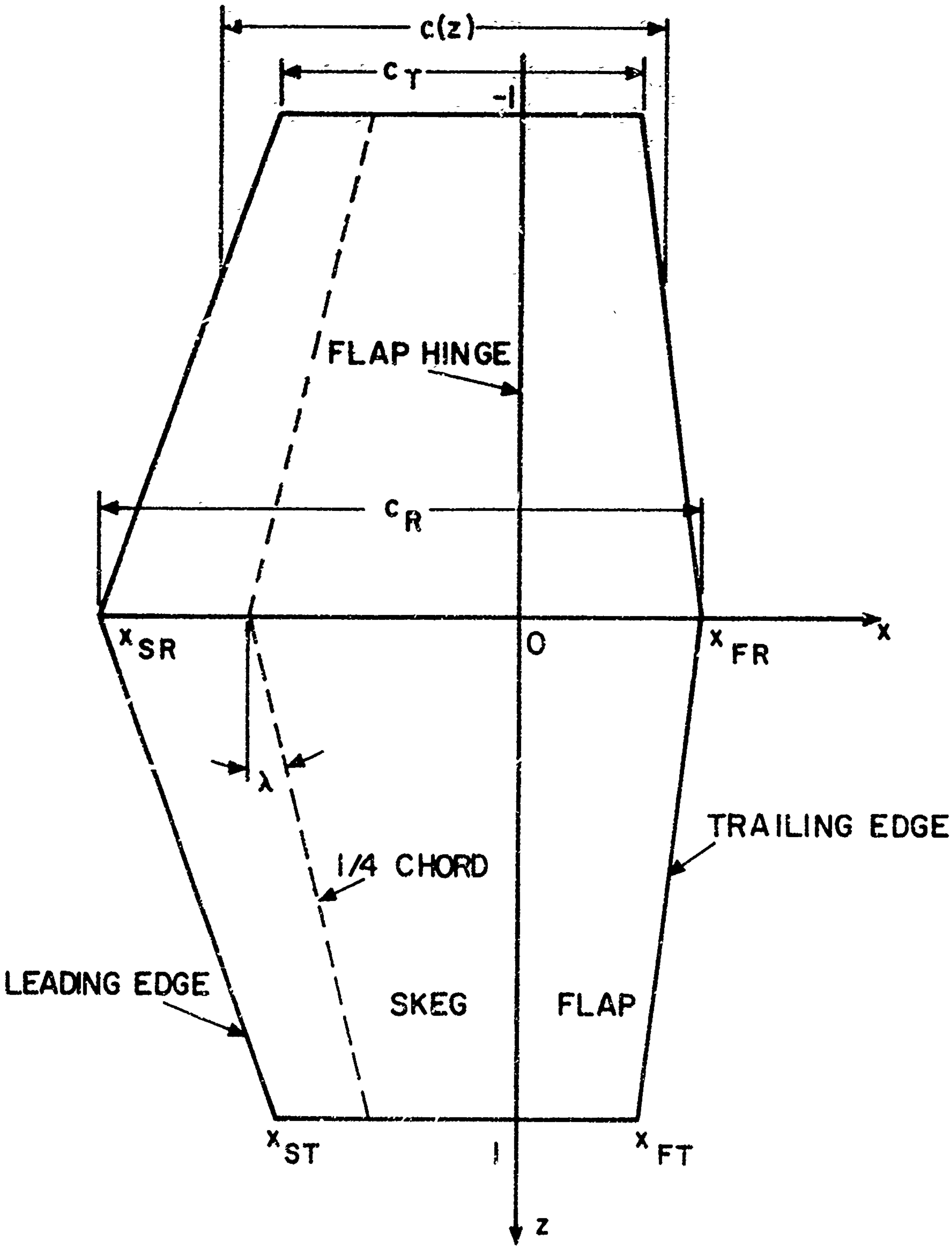

Fig. 1 Coordinate System and Notation for Planform Geometry

elements running out of the leading and trailing edges, which is inevitably a source of inaccuracy. This would be particularly objectionable in the tip region of a small flap.

As a result, the spanwise vortex lines are not purely bound vortices, since they include a component of vorticity parallel to the oncoming flow. However, as long as the accompanying system of trailing vortices is arranged in such a way that continuity of vorticity is preserved, this is an equally valid, discrete representation of a continuous vortex system.

It was decided to use a strictly linear lifting-surface theory, since an examination of results for two-dimensional airfoils with flaps [3] indicates that flap effectiveness is reduced due to viscous effects before any non-linear augment of lift becomes apparent. Consequently, the vortex system is located on a plane, even when the flap is deflected, and the influence of thickness on loading vanishes. One may then solve the problem of a rudder with zero flap deflection and unit angle of attack, and a separate problem of a rudder with zero angle of attack and unit flap deflection. The solution to any combination of angle of attack and flap deflection is then simply a linear combination of the preceding two results.

2. DISCRETE VORTEX ARRANGEMENT

The computer program is designed to accommodate any quadrilateral flapped control surface with a hinge axis normal to the flow, and with a tip parallel to the flow, as indicated in Fig. 1. The planform geometry is uniquely specified by the four nondimensional quantities tabulated below:

Symbol	Definition
a	Effective aspect ratio $\frac{(2s)^2}{A}$
f	Flap area ratio A_F/A
λ	Taper ratio c_T/c_R
Λ	Sweep angle of 1/4-chord

From these, we may obtain the coordinates of the four corners of the control surface. The coordinate system, as shown in Fig. 1, is located with the x-axis situated at the root section and the z-axis coincident with the flap hinge axis. The semispan, s, is taken to be unity, so that all length dimensions are nondimensionalized at the outset with respect to this quantity. The x-coordinates of the four corner points then become:

$$x_{FR} = \frac{3(1 - \lambda) + 4f(1 + \lambda)}{2a(\lambda + 1)} - \frac{1}{2} \tan \Lambda$$

$$x_{SR} = x_{FR} - \frac{4}{a(\lambda + 1)}$$

$$x_{FT} = \frac{3(\lambda - 1) + 4f(1 + \lambda)}{2a(\lambda + 1)} + \frac{1}{2} \tan \Lambda$$

$$x_{ST} = x_{FT} - \frac{4\lambda}{a(\lambda + 1)} \quad . \tag{2.1}$$

If we do not wish to have the flap hinge emerge from either the leading or trailing edge, it is necessary that the choice of input quantities be such that x_{FR} and $x_{FT} > 0$ and x_{SR} and $x_{ST} < 0$. If these conditions are not met, an error message is printed.

The two trapezoidal regions representing the skeg and flap may now be subdivided into a lattice of spanwise and trailing discrete vortex lines. An individual segment of a spanwise vortex, together with the two trailing vortices originating at the ends of the segment, forms a horseshoe vortex of constant strength, as illustrated in Fig. 2.

The complete lattice arrangement is shown in Fig. 3. The fineness of the grid is controlled by specifying a spanwise precision number, $I_V = 0$, 1, or 2, and a chordwise precision number, $I_H = 0$, 1, or 2. A zero precision number denotes the coarsest possible grid spacing, which is the one illustrated in Fig. 3.

The semispan is divided into $5I_V + 7$ chordwise panels of equal width. The panel nearest to the tip is further subdivided into 14 equal intervals, and this pattern is duplicated on the image side of the planform. The total number of chordwise strips over the span, I, for each precision number is as follows:

Precision Number I_V	Number of Chordwise Panels I
0	40
1	50
2	60

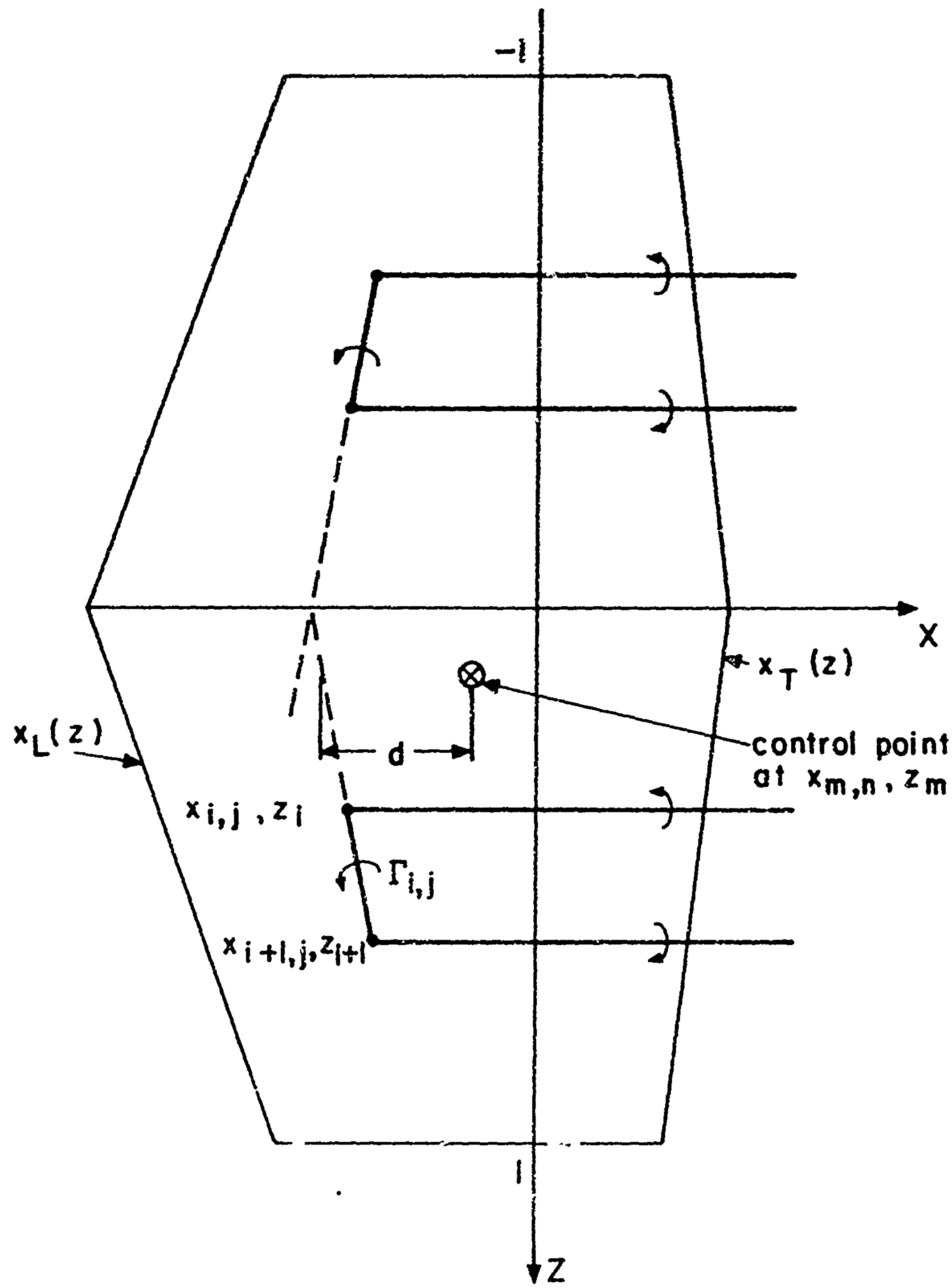

Fig. 2 Illustration of a Typical Horseshoe Vortex Element

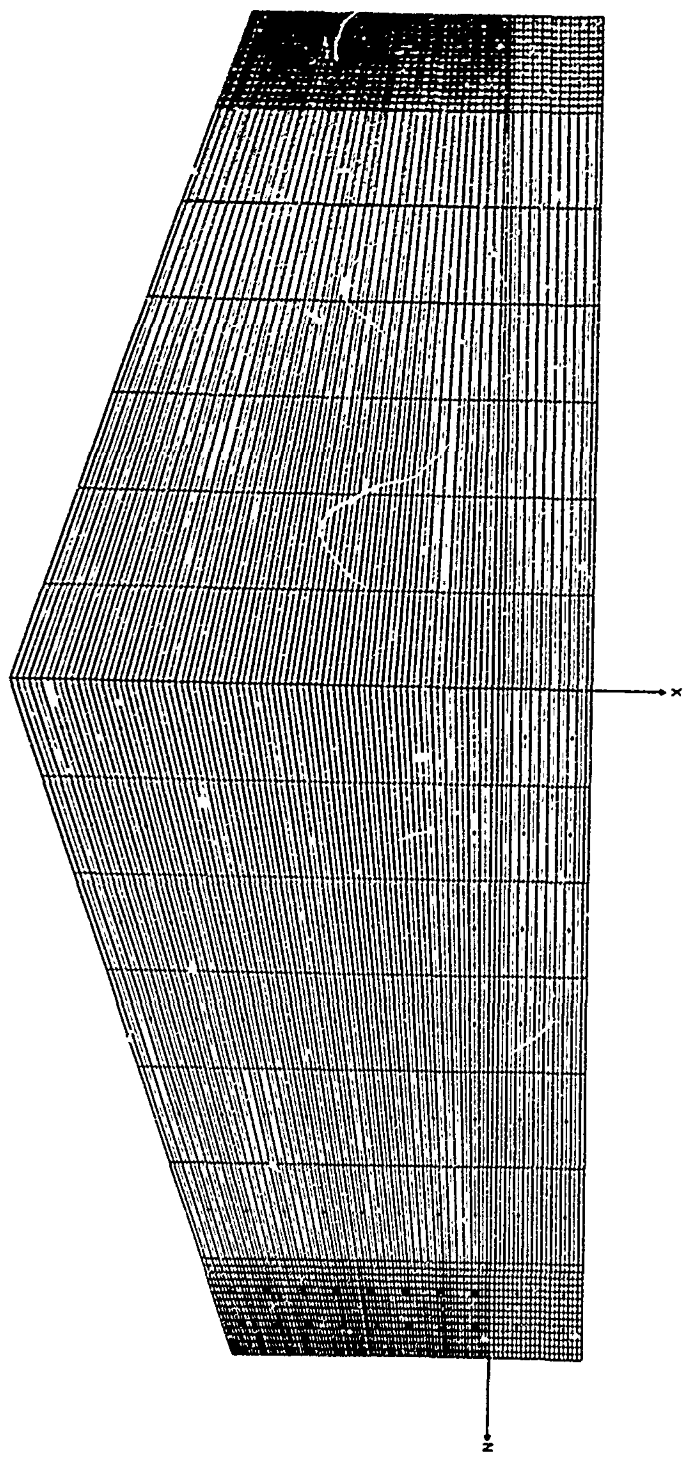

Fig. 3 Complete Lattice Arrangement Corresponding to Zero Precision Number

The total chord is divided into J spanwise panels in accordance with the specified horizontal precision number I_H,

$$J = 50 + 10\, I_H \quad . \tag{2.2}$$

In general, it is not possible to have the chordwise spacing the same on both the skeg and the flap. However, the two spacings will be very nearly equal if the number of panels on the flap, NF, is the integer closest to the flap area ratio times the total number of intervals over the chord,

$$NF \geq f \cdot J \quad . \tag{2.3}$$

The number of panels on the skeg, NS, is then:

$$NS = J - NF \quad . \tag{2.4}$$

The determination of NF and NS is internal to the computer program, based on the specified input value of f.

Velocities are computed at 80 control points distributed over the span and chord. Their spanwise placement is permanent, as indicated by small circles in Fig. 3. Their chordwise placement is arbitrary, and is specified as input data by the user. Spanwise vortex lines are placed in the middle of each panel. Each control point is located midway between adjacent spanwise and trailing vortex elements, which is essential in order for the discrete system to converge to the Canchy-Principal Value of the corresponding continuous singular integral. Thus the control points are placed on the panel boundaries.

To avoid errors due to edge effects, control points should be located at least 2 spaces away from the leading and trailing edges, and 4 spaces away from the tip. The choice of 8 spanwise and 10 chordwise stations follows from our experience with similar computing schemes for propellers [2]. Since the flap, when deflected, acts to some extent as an independent lifting

surface, it is important to include as many control points as possible over the flap chord, while avoiding the immediate vicinity of the hinge line. This requires an unusually large number of panels over the chord, and a flexible system of specifying control point locations.

This lattice arrangement, which concentrates at least half of the elements over the outer seventh of the span, is the result of considerable numerical experimentation. Lifting surfaces with trapezoidal planforms may, under certain circumferences, have a spanwise load distribution which falls to zero very abruptly at the tip. To obtain accurate results it is necessary to locate a sufficient number of control points very close to the tip. However, to avoid edge effects, as we have noted before, it is essential to have several grid spaces between the outboard control point and the tip. One must, therefore, have an extremely fine grid in this region. Since a relatively coarse spacing provides ample accuracy in the midspan region of the lifting surface, it would be an extreme waste of computer time to extend the fine grid over the entire planform.

3. CONTINUOUS AND DISCRETE CIRCULATION DISTRIBUTION

One could, in principle, solve for the circulation of each discrete spanwise vortex element necessary to satisfy the flow tangency boundary condition at each control point. However, this would require that the number of control points be equal to the number of vortex elements, and would result in the need to solve large systems of simultaneous equations. For zero precision number, for example, there would have to be 800 control points rather than 80, and there would be 800 simultaneous equations to solve.

We will, therefore, employ a modal approach, which greatly reduces the number of unknowns. The continuous distribution of circulation over the span and chord is assumed to be given by a series of known forms with unknown coefficients, following the classical work of Glauert [4]. The non-dimensional circulation distribution due to the angle of attack, $G^{(\alpha)}$, and flap deflection, $G^{(\delta)}$, is assumed to be given by the following series:

$$G^{(\alpha)}(x,z) = \frac{\gamma^{(\alpha)}(x,z)}{4U} = \sum_{k=1}^{K} \sum_{\ell=1}^{L-1} c_{k\ell}^{(\alpha)} f_k(\tilde{z})\, p_\ell(\tilde{s}) \tag{3.1}$$

$$G^{(\delta)}(x,z) = \frac{\gamma^{(\delta)}(x,z)}{4U} \quad \sum_{k=1}^{K} \sum_{\ell=1}^{L} c_{k\ell}^{(\delta)} f_k(\tilde{z})\, p_\ell(\tilde{s}) \; . \tag{3.2}$$

In the above equations $c_{k\ell}$ are unknown mode amplitudes, $f_k(\tilde{z})$ are the spanwise modes, and $p_\ell(\tilde{s})$ are the chordwise modes. The spanwise modes are given by the following expression:

$$f_k(\tilde{z}) = \sin[(2k - 1)\tilde{z}] \; , \tag{3.3}$$

where $\tilde{z}$ is the transformed spanwise coordinate

$$\tilde{z} = \cos^{-1}(-z) \ . \qquad (3.4)$$

The chordwise modes are

$$p_1(\tilde{s}) = \frac{2}{\pi c(z)} \left(\frac{1 + \cos \tilde{s}}{\sin \tilde{s}}\right) \qquad (3.5)$$

$$p_\ell(\tilde{s}) = \frac{4 \sin[(\ell-1)\tilde{s}]}{\pi c(z)} \qquad \ell = 2, 3, \ldots, L - 1 \qquad (3.6)$$

$$p_L(\tilde{t}) = \frac{2}{\pi x_T(z)} \left(\frac{1 + \cos \tilde{t}}{\sin \tilde{t}}\right) \qquad (3.7)$$

where

$$\tilde{s} = \cos^{-1}\left[1 - \frac{2(x - x_L(z))}{c(z)}\right] \qquad (3.8)$$

$$\tilde{t} = \cos^{-1}\left[1 - \frac{2x}{x_T(z)}\right] \ . \qquad (3.9)$$

The last chordwise mode, corresponding to $\ell = L$, contains a square-root singularity at the leading edge of the flap and is, therefore, omitted in (3.1). The first six spanwise and chordwise modes are plotted in Fig. 4. One can readily see from Fig. 4 that control points must be located very near the tip in order to resolve the fifth and sixth spanwise modes.

The chordwise modes may be integrated to obtain the total circulation around any element of chord length:

$$P_1(\tilde{s}) = \int p_1(\tilde{s})dx = \frac{1}{\pi}(\tilde{s} + \sin \tilde{s}) \qquad (3.10)$$

$$P_2(\tilde{s}) = \int p_2(\tilde{s})dx = \frac{1}{\pi}\left(\tilde{s} - \frac{\sin 2\tilde{s}}{2}\right) \qquad (3.11)$$

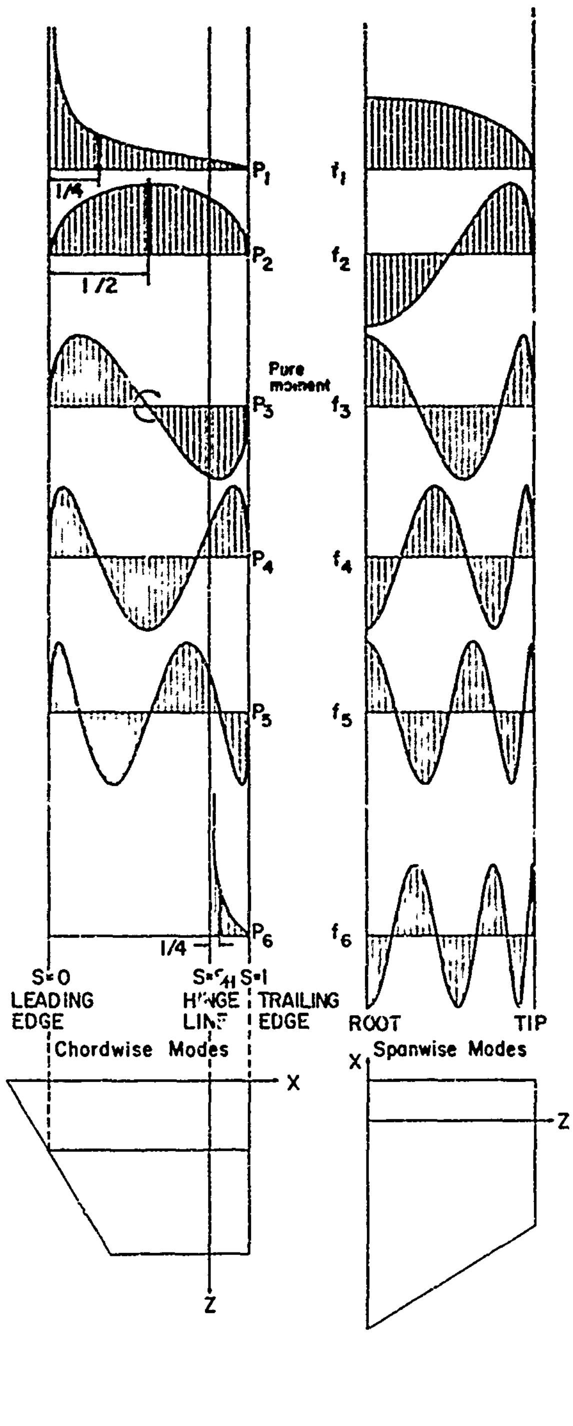

Fig. 4 Chordwise and Spanwise Mode Shapes

$$P_\ell(\tilde{s}) = \int p_\ell(\tilde{s})dx = \frac{2}{\pi}\left(\frac{\sin(\ell-2)\tilde{s}}{2(\ell-2)} - \frac{\sin \ell\tilde{s}}{2\ell}\right) \qquad \ell = 2, 3, \ldots, L-1 \tag{3.12}$$

$$P_L(\tilde{t}) = \int p_L(\tilde{t})dx = \frac{1}{\pi}(\tilde{t} + \sin\tilde{t}) \quad . \tag{3.13}$$

The total circulation around any spanwise station due to each mode is obtained by substituting the leading and trailing edges as limits in the preceding integrals. It, therefore, follows that

$$\int_{x_L(z)}^{x_T(z)} p_1(\tilde{s})dx = 1$$

$$\int_{x_L(z)}^{x_T(z)} p_2(\tilde{s})dx = 1$$

$$\int_{x_L(z)}^{x_T(z)} p_\ell(\tilde{s})dx = 0 \qquad \ell = 2, \ldots, L-1$$

$$\int_{0}^{x_T(z)} p_L(\tilde{t})dx = 1 \ . \tag{3.14}$$

We can now combine (3.14) with the spanwise modes to obtain an expression for the spanwise circulation distribution

$$\Gamma^{(\alpha)}(z) = \int_{x_L(z)}^{x_T(z)} \gamma^{(\alpha)}(x,z)dx = 4U \sum_{k=1}^{K} (c_{k1}^{(\alpha)} + c_{k2}^{(\alpha)}) f_k(\tilde{z}) . \tag{3.15}$$

$$\Gamma^{(\delta)}(z) = \int_{x_L(z)}^{x_T(z)} \gamma^{(\delta)}(x,z)dx = 4U \sum_{k=1}^{K} (c_{k1}^{(\delta)} + c_{k2}^{(\delta)} + c_{kL}^{(\delta)}) f_k(\tilde{z}) \ . \tag{3.16}$$

We can now obtain the circulation strengths of each discrete spanwise element corresponding to each mode of unit amplitude. The circulation must be, of course, constant over the span of the element. We chose to make this value correspond to that of the continuous distribution at the midspan of the element. Consequently, the spanwise mode value is obtained by substituting the value of $\tilde{z}$ corresponding to the midspan of the element in question into (3.3). The circulation is then obtained by multiplying this value from (3.5) by the integral of the particular chordwise mode over one chordwise interval from (3.10) - (3.13). The sum of the strengths of the spanwise vortices over any chordwise panel will, therefore, be equal to the total circulation around the midspan of the panel in the continuous case.

The circulation of the two trailing vortices shed from the ends of each spanwise vortex segment must then have the same magnitude with an appropriate algebraic sign. Finally, since corresponding elements on the image portion of the lifting surface have the same strength, this computation needs to be made only over the semispan.

An alternative procedure for determining individual vortex strengths is a method originated by Faulkner [1]. The relative vortex strengths corresponding to any chordwise mode are obtained by requiring that the downwash at each panel boundary be exact in two-dimensional flow. The results are given in Table 1 for 8 chordwise panels, and in Table 2 for 50 chordwise panels. The only significant differences occur in the first

FAULKNER SOLUTION

	J=1	J=2	J=3	J=4	J=5
N= 1	0.392761	0.072006	0.126011	0.146058	0.129591
N= 2	0.183289	0.123367	0.154209	0.068072	-0.069119
N= 3	0.126892	0.147079	0.110310	-0.065429	-0.159381
N= 4	0.096130	0.157547	0.039387	-0.148702	-0.076562
N= 5	0.074768	0.157547	-0.039387	-0.148702	0.076562
N= 6	0.057678	0.147079	-0.110310	-0.065429	0.159381
N= 7	0.042297	0.123367	-0.154209	0.068072	0.069119
N= 8	0.026184	0.072006	-0.126011	0.146058	-0.129591

MODE INTEGRATION

	J=1	J=2	J=3	J=4	J=5
N= 1	0.440596	0.072147	0.122816	0.138168	0.116676
N= 2	0.168402	0.123354	0.152848	0.068580	-0.061543
N= 3	0.118774	0.147018	0.109588	-0.062279	-0.151446
N= 4	0.090538	0.157431	0.039160	-0.144470	-0.073452
N= 5	0.070323	0.157431	-0.039160	-0.144470	0.073452
N= 6	0.053698	0.147018	-0.109588	-0.062279	0.151446
N= 7	0.038158	0.123354	-0.152848	0.068580	0.061543
N= 8	0.019511	0.072147	-0.122816	0.138168	-0.116676

Table 1. Relative Vortex Strength for Eight Chordwise Intervals. The mode index is J and the vortex element index is N.

	MODE INTEGRATION					FAULKNER'S SOLUTION				
	J = 1	J = 2	J = 3	J = 4	J = 5	J = 1	J = 2	J = 3	J = 4	J = 5
N= 1	0.179461	0.004773	0.009317	0.013416	0.016987	0.159178	0.004759	0.009328	0.013493	0.017118
N= 2	0.073479	0.008644	0.016232	0.021842	0.024799	0.070785	0.008642	0.016247	0.021887	0.024900
N= 3	0.055791	0.011079	0.019929	0.024773	0.024652	0.058480	0.011090	0.019945	0.024808	0.024710
N= 4	0.046534	0.012992	0.022317	0.025391	0.021357	0.048222	0.012993	0.022331	0.025416	0.021385
N= 5	0.040553	0.014566	0.023979	0.024597	0.016452	0.041735	0.014567	0.023990	0.024604	0.016460
N= 6	0.036257	0.015928	0.024840	0.022817	0.010760	0.037152	0.015930	0.024852	0.022825	0.010763
N= 7	0.032965	0.017122	0.025333	0.020369	0.004831	0.033674	0.017123	0.025342	0.020374	0.004814
N= 8	0.030328	0.018191	0.025447	0.017445	-0.001003	0.030905	0.018182	0.025454	0.017447	-0.001028
N= 9	0.028147	0.019127	0.025241	0.014194	-0.006483	0.028636	0.019129	0.025248	0.014194	-0.006513
N=10	0.026299	0.019976	0.024765	0.010737	-0.011428	0.026719	0.019977	0.024771	0.010733	-0.011462
N=11	0.024703	0.020741	0.024055	0.007168	-0.015716	0.025070	0.020742	0.024060	0.007162	-0.015752
N=12	0.023303	0.021430	0.023140	0.003568	-0.019263	0.023628	0.021431	0.023145	0.003560	-0.019200
N=13	0.022058	0.022051	0.022047	0.000004	-0.022019	0.022349	0.022051	0.022051	-0.000006	-0.022057
N=14	0.020940	0.022639	0.020796	-0.003467	-0.023963	0.021203	0.022639	0.020800	-0.003478	-0.024000
N=15	0.019926	0.023109	0.019407	-0.006796	-0.025094	0.020166	0.023108	0.019411	-0.006809	-0.025130
N=16	0.018999	0.023552	0.017897	-0.009940	-0.025431	0.019219	0.023553	0.017900	-0.009954	-0.025465
N=17	0.018145	0.023946	0.016281	-0.012864	-0.025909	0.018349	0.023946	0.016293	-0.012879	-0.025041
N=18	0.017354	0.024290	0.014572	-0.015535	-0.023876	0.017543	0.024290	0.014574	-0.015551	-0.023905
N=19	0.016616	0.024597	0.012783	-0.017928	-0.022091	0.016793	0.024598	0.012786	-0.017544	-0.022117
N=20	0.015925	0.024839	0.010928	-0.020018	-0.019723	0.016092	0.024839	0.010925	-0.020036	-0.019745
N=21	0.015275	0.025047	0.009016	-0.021789	-0.016849	0.015432	0.025047	0.009017	-0.021806	-0.016867
N=22	0.014661	0.025212	0.007258	-0.023223	-0.013552	0.014810	0.025213	0.007060	-0.023241	-0.013567
N=23	0.014077	0.025335	0.005066	-0.024309	-0.009922	0.014219	0.025336	0.005067	-0.024327	-0.009933
N=24	0.013522	0.025417	0.003050	-0.025038	-0.006051	0.013657	0.025418	0.003050	-0.025057	-0.006057
N=25	0.012991	0.025459	0.001018	-0.025404	-0.002033	0.013120	0.025458	0.001018	-0.025423	-0.002035
N=26	0.012481	0.025459	-0.001018	-0.025404	0.002033	0.012606	0.025458	-0.001018	-0.025423	0.002035
N=27	0.011991	0.025417	-0.003050	-0.025038	0.006051	0.012111	0.025418	-0.003050	-0.025057	0.006057
N=28	0.011519	0.025335	-0.005066	-0.024309	0.009922	0.011634	0.025336	-0.005067	-0.024327	0.009933
N=29	0.011059	0.025212	-0.007058	-0.023223	0.013552	0.011172	0.025213	-0.007060	-0.023241	0.013567
N=30	0.010614	0.025047	-0.009016	-0.021789	0.016849	0.010724	0.025047	-0.009017	-0.021806	0.016867
N=31	0.010181	0.024839	-0.010928	-0.020018	0.019723	0.010288	0.024839	-0.010929	-0.020036	0.019745
N=32	0.009758	0.024597	-0.012783	-0.017928	0.022091	0.009863	0.024598	-0.012786	-0.017944	0.022117
N=33	0.009343	0.024290	-0.014572	-0.015535	0.023876	0.009446	0.024290	-0.014574	-0.015551	0.023905
N=34	0.008936	0.023946	-0.016281	-0.012864	0.025909	0.009037	0.023946	-0.016283	-0.012879	0.025041
N=35	0.008534	0.023552	-0.017897	-0.009543	0.025431	0.008625	0.023553	-0.017900	-0.009954	0.025465
N=36	0.008137	0.023109	-0.019407	-0.006796	0.025094	0.008237	0.023109	-0.019411	-0.006808	0.025130
N=37	0.007743	0.022639	-0.020796	-0.003467	0.023963	0.007842	0.022639	-0.020800	-0.003478	0.024000
N=38	0.007351	0.022051	-0.022047	0.000004	0.022019	0.007450	0.022051	-0.022051	-0.000006	0.022057
N=39	0.006959	0.021430	-0.023140	0.003569	0.019263	0.007058	0.021431	-0.023145	0.003560	0.019200
N=40	0.006564	0.020741	-0.024055	0.007169	0.015716	0.006664	0.020742	-0.024060	0.007162	0.015752
N=41	0.006166	0.019976	-0.024765	0.010737	0.011428	0.006268	0.019977	-0.024771	0.010733	0.011462
N=42	0.005762	0.019127	-0.025241	0.014194	0.006483	0.005865	0.019129	-0.025248	0.014194	0.006513
N=43	0.005349	0.018191	-0.025447	0.017445	0.001003	0.005455	0.018182	-0.025454	0.017447	0.001028
N=44	0.004921	0.017122	-0.025333	0.020369	-0.004831	0.005032	0.017123	-0.025342	0.020374	-0.004814
N=45	0.004475	0.015979	-0.024842	0.022817	-0.010749	0.004592	0.015930	-0.024850	0.022829	-0.010763
N=46	0.004003	0.014566	-0.023979	0.024587	-0.016452	0.004128	0.014567	-0.023990	0.024604	-0.016460
N=47	0.003491	0.012982	-0.022317	0.025391	-0.021357	0.003629	0.012993	-0.022331	0.025416	-0.021385
N=48	0.002917	0.011079	-0.019929	0.024773	-0.024652	0.003078	0.011090	-0.019945	0.024808	-0.024710
N=49	0.002229	0.008644	-0.016232	0.021842	-0.024799	0.002437	0.008642	-0.016247	0.021887	-0.024900
N=50	0.001208	0.004773	-0.009317	0.013416	-0.016980	0.001608	0.004759	-0.009328	0.013493	-0.017118

Table 2. Relative Vortex Strength for Fifty Chordwise Intervals. The mode index is J and the vortex element index is N.

chordwise mode near the leading and trailing edges, and both methods result in essentially identical final values of lift distribution. However, the Faulkner method requires a greater amount of computation, since the relative panel widths on the skeg and flap are functions of spanwise position. For zero precision number, the Faulkner method would require the solution of 120 different sets of simultaneous equations, each with 50 unknowns. Without the complication of the flap, the Faulkner procedure for obtaining relative vortex strengths would be much simpler, since the relative vortex strengths could be pre-computed.

4. COMPUTATION OF INDUCED VELOCITIES

The lattice arrangement as described in Section 2 results in a set of discrete, skewed horseshoe vortex elements, as shown in Fig. 2. Consider a particular horseshoe element consisting of a spanwise vortex of strength Γ extending from (x_1,z_1) to (x_2,z_2), joined by semi-infinite trailing vortices of strength Γ starting at (x_2,z_2) and $-\Gamma$ starting at (x_1,z_1). For each such element located in the interval $0 \leq z \leq 1$, there will be a corresponding image element of the same strength extending from $(x_2,-z_2)$ to $(x_1,-z_1)$. The trailing vortex shed at $(x_2,-z_2)$ will have a strength $-\Gamma$, while the vortex shed from $(x_1,-z_1)$ will have a strength of $+\Gamma$.

Let us first consider the spanwise vortex segment. Defining (ξ,ζ) as the coordinates of a general point on the vortex, and (x,z) as the coordinates of the control point, the velocity may be written in accordance with the law of Biot-Savart as follows:

$$\frac{4\pi\, v^{(s)}(x,z)}{\Gamma} = \int_{x_1,z_2}^{x_2,z_2} \frac{(x-\xi)d\zeta - (z-\zeta)d\xi}{[(x-\xi)^2 + (z-\zeta)^2]^{3/2}} \quad . \tag{4.1}$$

Along the vortex, we have:

$$t = \frac{d\xi}{d\zeta} = \frac{x_2-x_1}{z_2-z_1} = \text{const} \quad , \tag{4.2}$$

so that (4.1) may be expressed in terms of the variable ζ alone and readily integrated to give the result:

$$\frac{4\pi\, v^{(s)}(x,z)}{\Gamma} = \frac{2a\zeta+b}{2d\sqrt{a\zeta^2+b\zeta+c}} \Bigg|_{z_1}^{z_2}$$

where

$$a = 1+t^2$$

$$e = x-x_1+tz_1$$

$$b = -2(et+z)$$

$$c = e^2+z^2$$

$$d = e-tz \quad . \tag{4.3}$$

Equation (4.3) is not suitable for numerical computation if d becomes small. As is evident from Fig. 2, d is the horizontal distance between the control point and the spanwise vortex line or its extension. For the vortex arrangement shown in Fig. 3, d can never be less than approximately one half the chordwise grid spacing for vortex elements occupying the semi-span interval $0 \leq z \leq 1$. The distance d will only become small enough to cause problems if the aspect ratio is extremely high. For this situation, the limiting form of (4.1) valid for $d \ll 1$ is:

$$\frac{4\pi \, v^{(s)}(x,z)}{\Gamma} = 2\sqrt{a}\left[\frac{1}{d} - \frac{2d}{(2az_1+b)^2} - \frac{2d}{(2az_2+b)^2}\right] \quad , \tag{4.4}$$

provided $z_1 < z < z_2$. In that case, the velocity approaches that of an infinite vortex as given by the first term in (4.4). The second and third terms represent small corrections to the result for an infinite vortex. It has been found by numerical experimentation that round-off error is minimized if (4.4) is used for $|d| < 0.002$.

If z is not in the interval $z_1 < z < z_2$, the first term of (4.4) disappears, and the velocity tends to zero as $d \to 0$. If (4.3) is used in this case, catastrophic round-off error can occur. This is because the integral becomes very large, but independent of ζ. Hence, the integral

from z_1 to z_2 becomes the small difference between the two large numbers.

This situation does not occur in practice for elements over the semi-span. However, due to the inclination of the spanwise vortex lines, it is evident from Fig. 3. that a control point could easily be aligned with the extension of an image vortex segment located in the interval $-1 \leq z \leq 0$. This can result in seemingly random errors which come and go with minor changes in grid spacing or planform. This problem is eliminated entirely if the velocity is set to zero for $|d| < 0.002$ provided z is outside the interval $z_1 < z < z_2$. Inclusion of the small correction similar to the second term of (4.4) makes no difference, and is therefore an unnecessary complication.

The velocity induced by the two trailing vortices is:

$$\frac{4\pi\, v^{(t)}(x,z)}{\Gamma} = (z-z_1) \int_{x_1}^{\infty} \frac{d\xi}{[(x-\xi)^2 + (z-z_1)^2]^{3/2}}$$

$$- (z-z_2) \int_{x_2}^{\infty} \frac{d\xi}{[(x-\xi)^2 + (z-z_2)^2]^{3/2}}$$

$$= \frac{1}{z-z_1}\left[\frac{x-x_1}{\sqrt{(x-x_1)^2 + (z-z_1)^2}} + 1\right] - \frac{1}{z-z_2}\left[\frac{x-x_2}{\sqrt{(x-x_2)^2 + (z-z_2)^2}} + 1\right] \tag{4.5}$$

Since the trailing vortices are all parallel, the round-off error situation is much simpler than for the spanwise vortices. Difficulties could only be encountered for aspect ratios far below those of practical interest. Equation (4.5) may therefore be used for all elements.

The total velocity induced by a horseshoe element is the sum of either (4.3) or (4.4) and (4.5). The contribution of corresponding image elements

may then be obtained by repeating this computation following the substitution:

$$x_1 \to x_2$$
$$z_1 \to -z_2$$
$$x_2 \to x_1$$
$$z_2 \to -z_1 \qquad (4.6)$$

which results in the correct algebraic sign for each of the individual elements. We shall use the notation $v_{m,n,i,j}$ to denote the velocity induced at the control point located at (z_m, x_n) by the complete unit strength horseshoe element located between $(z_i, x_{i,j})$ and $(z_{i+1}, x_{i+1,j})$ together with its image.

The FORTRAN function HSVEL listed in the appendix performs this calculation.

The strength of the (i,j)'th vortex element corresponding to the k'th spanwise and ℓ'th chordwise modes of unit amplitude is

$$f_k(\tilde{z}_i)\, P_\ell(\tilde{s}_{i,j}) \ , \qquad (4.7)$$

where $\tilde{z}_i$ is the transformed coordinate of the midspan of the element

$$\tilde{z}_i = \cos^{-1}\left(-\frac{(z_i + z_{i+1})}{2}\right) \ , \qquad (4.8)$$

and $P_\ell(\tilde{s}_{i,j})$ is the integral of the chord load function obtained by substituting the x-coordinates of the leading and trailing edges of the midspan of the (i,j)'th element as limits of integration in (3.14).

The velocity induced at the (m,n)'th control point by the (k,ℓ)'th mode of unit amplitude is, therefore, obtained by summing the product of the mode strengths from (4.7) with the velocities for unit circulation obtained from (4.3) - (4.5) over all I × J horseshoe elements:

$$v_{m,n,k,\ell} = \sum_{i=1}^{I} f_k(\tilde{z}_i) \sum_{j=1}^{J} P_\ell(\tilde{s}_{ij}) v_{m,n,i,j} \ . \tag{4.9}$$

Since the contribution of the image is included in $v_{m,n,i,j}$, the summation in (4.9) is only over the elements in the semi-span interval $0 \le z \le 1$.

We can now write the final expression for the velocity induced at the (m,n)'th control point in terms of the unknown mode amplitudes $c_{k,\ell}$:

$$V_{m,n} = \sum_{k=1}^{K} \sum_{\ell=1}^{L} c_{k,\ell} \, v_{m,n,k,\ell} \ . \tag{4.10}$$

Equation (4.10) represents a set of simultaneous equations for the mode amplitude coefficients, once the values of $V_{m,n}$ are prescribed by the boundary conditions of the problem. The mode amplitude coefficients corresponding to zero flap deflection and unit angle of attack, $c_{k,\ell}^{(\alpha)}$, are obtained by solving (4.10) with $V_{m,n} = +1$ for all values of (m,n). Similarly, the mode amplitude coefficients for zero angle of attack and unit flap deflection are obtained by setting $V_{mn} = 0$ for all values of (m,n) corresponding to control points on the skeg, and $V_{mn} = +1$ for all values of (m,n) corresponding to control points on the flap.

If the number of modes is equal to the number of control points, the boundary condition may be satisfied exactly at all the control points. If the number of modes is less than this, (4.10) may be solved by least squares to provide the closest possible fit at all the control points. The latter approach is preferred, since the higher modes amplitudes are generally of

questionable accuracy. For this application we solve (4.10) for K·L unknown mode amplitude coefficients by least squares through 80 control points.

5. COMPUTATION OF FORCES

Lift and induced drag may be obtained most directly from the spanwise circulation distribution given in (3.15) and (3.16), employing the well-known results of classical lifting-line theory [4]. The local lift coefficient per unit angle of attack is:

$$C_{L\alpha}(z) = \frac{-\rho U\Gamma^{(\alpha)}(z)}{\frac{1}{2}\rho U^2 c(z)} = \frac{8}{c(z)} \sum_{k=1}^{K} f_k(\tilde{z})\{c_{k1}^{(\alpha)} + c_{k2}^{(\alpha)}\} \quad , \tag{5.1}$$

noting that the coefficients $c_{k\ell}$ and the circulation Γ have been obtained from (4.10) for an angle of attack of unity. Similarly, the lift coefficient due to unit flap deflction is:

$$C_{L\delta}(z) = \frac{8}{c(z)} \sum_{k=1}^{K} f_k(\tilde{z})\{c_{k1}^{(\delta)} + c_{k2}^{(\delta)} + c_{kL}^{(\delta)}\} \quad . \tag{5.2}$$

Overall lift coefficients are obtained by multiplying (5.1) and (5.2) by the local chord, c(z), integrating over the span, and dividing by the area of the lifting surface. Since only the first spanwise mode contributes, we obtain the result:

$$C_{L\alpha} = \pi a(c_{11}^{(\alpha)} + c_{12}^{(\alpha)})$$

$$C_{L\delta} = \pi a(c_{11}^{(\delta)} + c_{12}^{(\delta)} + c_{1L}^{(\delta)}) \quad , \tag{5.3}$$

where a is the effective aspect ratio.

The induced drag coefficient, in accordance with lifting line theory, may be written as follows in terms of the present notation:

$$C_{Di\alpha} = \frac{C_{L\alpha}^2}{\pi a} [1 + \sum_{k=2}^{K} (2k-1) \{\frac{c_{k1}^{(\alpha)}+c_{k2}^{(\alpha)}}{c_{11}^{(\alpha)}+c_{12}^{(\alpha)}}\}^2]$$

$$C_{Di\delta} = \frac{C_{L\delta}^2}{\pi a} [1 + \sum_{k=}^{K} (2k-1) \{\frac{c_{k1}^{(\delta)}+c_{k2}^{(\delta)}+c_{kL}^{(\delta)}}{c_{11}^{(\delta)}+c_{12}^{(\delta)}+c_{1L}^{(\delta)}}\}^2] \quad . \tag{5.4}$$

The efficiencies $\eta^{\alpha,\delta}$ of the lifting-surface are defined as the reciprocals of the quantities in square brackets in (5.4), and are equal to one if the spanwise circulation coefficients are zero for k>1.

To obtain the chordwise position of the center of pressure at any spanwise location, we must obtain the first moments of the chordwise mode functions, p_ℓ.

$$M_1 = \int_{x_L}^{x_T} x\cdot p_1(\tilde{s})\ dx = x_L(z) + \frac{c(z)}{4}$$

$$M_2 = \int_{x_L}^{x_T} x\cdot p_2(\tilde{s})\ dx = x_L(z) + \frac{c(z)}{2}$$

$$M_3 = \int_{x_L}^{x_T} x\cdot p_3(\tilde{s})\ dx = -\frac{c(z)}{4}$$

$$M_\ell = \int_{x_L}^{x_T} x\cdot p_\ell(\tilde{s})\ dx = 0 \qquad \text{for } \ell = 4,\ldots L-1$$

$$M_L = \int_{0}^{x_T} x\cdot p_L(\tilde{t})\ dx = \frac{X_T(z)}{4} \quad . \tag{5.5}$$

The results for M_1, M_2 and M_L can be readily indentified as the positions of the center of pressure of these modes, remembering that the origin of the coordinate system is at the flap hinge, rather than at the leading edge. The third chordwise mode contributes a pure moment, while the remaining modes contribute neither force nor moment.

The local distance of the center of pressure resulting from the joint effect of all the modes is expressed as a fraction of the local chord from the hinge line as follows:

$$\frac{x_H^{(\alpha)}(z)}{c(z)} = \frac{1}{c(z)} \frac{\sum\limits_{k=1}^{K} f_k(\tilde{z}) \sum\limits_{\ell=1}^{L-1} c_{k,\ell}^{(\alpha)} M_\ell}{\sum\limits_{k=1}^{K} f_k(\tilde{z}) \sum\limits_{\ell=1}^{L-1} c_{k,\ell}^{(\alpha)} P_\ell}$$

$$\frac{x_H^{(\delta)}(z)}{c(z)} = \frac{1}{c(z)} \frac{\sum\limits_{k=1}^{K} f_k(z) \sum\limits_{\ell=1}^{L} c_{k,}^{(\delta)} M_\ell}{\sum\limits_{k=1}^{K} f_k(z) \sum\limits_{\ell=1}^{L} c_{k,}^{(\delta)} P_\ell} \quad . \tag{5.6}$$

Distance between the local center of pressure and the leading edge as a function of local chord can be easily found from (5.6) as:

$$\frac{x_{LE}^{(\alpha)}(z)}{c(z)} = 1 - \frac{1}{c(z)} [x_T(z) - x_H^{(\alpha)}(z)]$$

$$\frac{x_{LE}^{(\delta)}(z)}{c(z)} = 1 - \frac{1}{c(z)} [x_T(z) - x_H^{(\delta)}(z)] \quad . \tag{5.7}$$

Finally, the resultant chordwise position of the center of pressure relative to the flap hinge line can be obtained by integration over the semi-span,

$$\frac{\bar{x}_H^{(\alpha)}}{\bar{c}} = \frac{1}{\bar{c}\, C_{L\alpha}} \int_0^1 x_H^{(\alpha)}(z)\; C_{L\alpha}(z)\; c(z)dz$$

$$\frac{\bar{x}_H^{(\delta)}}{\bar{c}} = \frac{1}{\bar{c}\, C_{L\alpha}} \int_0^1 x_H^{(\delta)}(z)\; C_{L\delta}(z)\; c(z)dz \quad . \tag{5.8}$$

This integration is performed numerically, using ten equally spaced stations and an integration formula which has been developed for functions with a square-root singularity in slope at the tip [2].

The preceding results may be combined to generate lift, drag and moment characteristics for any set of combinations of angle of attack and flap deflection. By adding an empirical viscous drag term of the form:

$$C_{DV} = 0.0085 + 0.0166\; C_L^{\,2} \quad , \tag{5.9}$$

a realistic approximation to the characterists of a flapped control surface can be made, provided, of course, that stall does not occur. The constants appearing in (5.9) were obtained from experimental airfoil data with "standard roughness" given in [3]. A sample tabulation of this type is given in Appendix 3.

6. TESTS OF PROGRAM ACCURACY

The effect of the spanwise and chordwise grid spacing on computed lift-slope for a typical control surface is given in Table 3. Variations with precision numbers are quite small, and it may be concluded that zero precision numbers are satisfactory for planform shapes similar to the case examined.

Table 3

Variations of Parameters with Extreme Precision Numbers

I_V	I_H	$C_{Di\alpha}$	$C_{Di\delta}$	$C_{L\alpha}$	$C_{L\delta}$	η^{α}	η^{δ}
0	0	0.114	0.116	3.138	1.776	0.996	0.984
0	2	0.114	0.116	3.132	1.877	0.996	0.980
2	0	0.114	0.116	3.101	1.756	0.995	0.980
$a = 2.8$		$\Lambda = 15^{\circ}$		$f = 0.2$		$\lambda = 0.6$	

Convergence of the solution with increasing numbers of elements is a necessary but obviously not sufficient test of program accuracy. Fortunately, the results for zero flap deflection may be compared with corresponding solutions obtained by other current numerical lifting-surface theory techniques. A recent publication by Langan and Wang [5] is particularly helpful in this regard. This reference compares the spanwise distributions of lift for a tapered wing of aspect ratio 5 obtained by fifteen different lifting-surface computer programs. Fig. 5 shows the results of the present program

plotted on a reproduction of Langan and Wang's Fig. 13 which are in excellent agreement with the average results of the fifteen programs compared in [5]. The overall lift coefficient obtained by the present program for this example is 4.106 which agrees exactly wi. the results given in [5] obtained by the Tulinius program! Induced drag was also found to be in good agreement.

A comparison was also made of the lift coefficient of a rectangular planform of unit aspect ratio. Watkins, Woolston, and Cunningham in a 1959 report [6], cite the following values obtained from several sources, to which we have added the results from the present program:

Source	$C_{L\alpha}$
Jones (low aspect ratio limit)	1.571
Lawrence	1.400
Hsu	1.497
Watkins-Woolston-Cunningham	1.455
Present Program	1.508

As a further check in the low aspect ratio range, J. Dulmovits of the Grumman Aircraft Engineering Corporation kindly offered to run his program for a tapered planform of effective aspect ratio 2.8. He obtained a lift slope of 3.140, which agrees almost exactly with a value of 3.138 obtained by the present program.

A test of the portion of the program dealing with the flap was made by running a rectangular planform of aspect ratio 60, to provide an essentially two-dimensional result. The exact solution in this case, as given in [7], is

$$\frac{C_{L\delta}}{C_{L\alpha}} = \frac{[(\pi-\tilde{s}_H) + \sin(\pi-\tilde{s}_H)]}{\pi} \qquad (6.1)$$

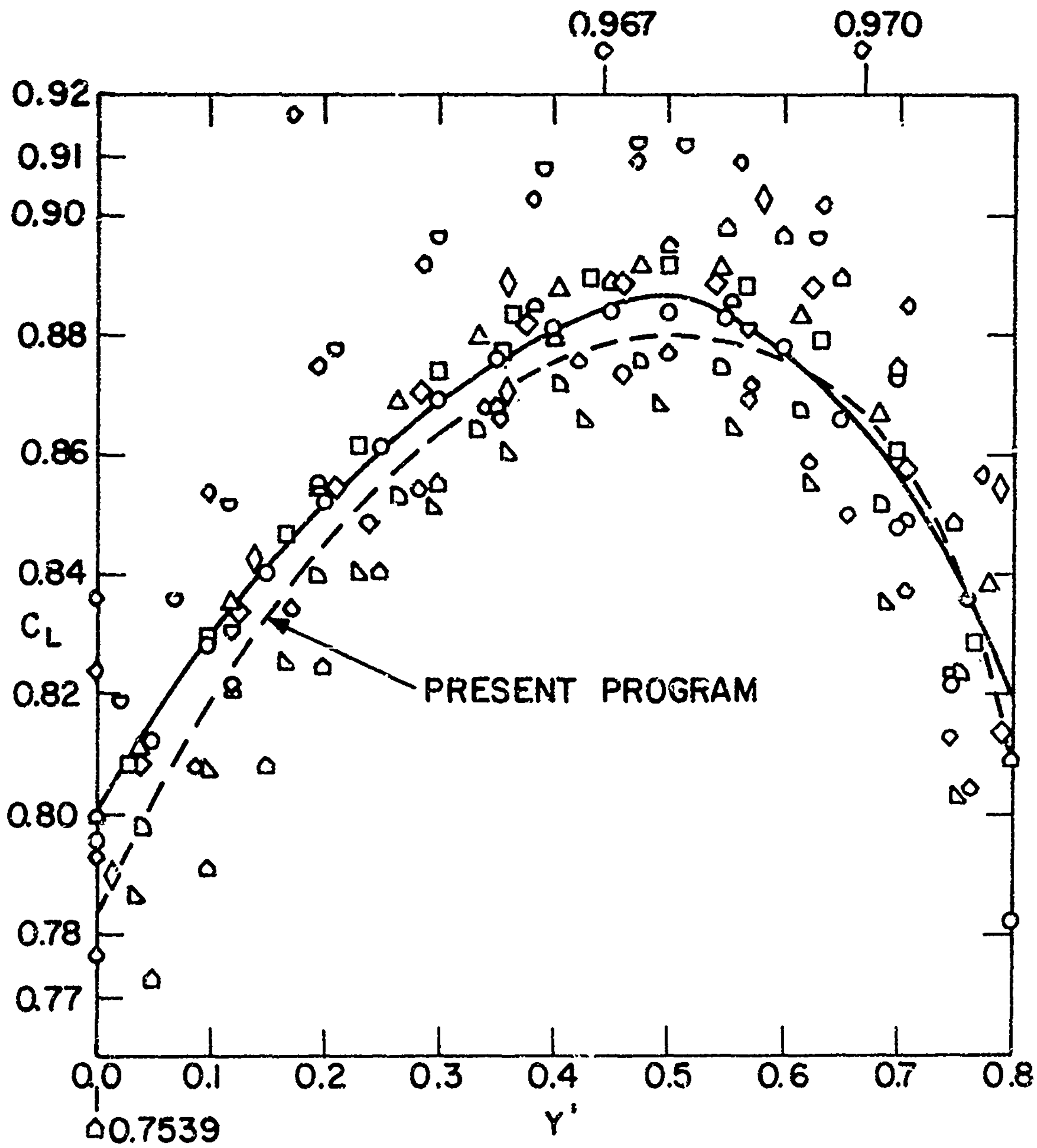

Fig. 5 Spanwise Lift Distribution Obtained by Present Program Superimposed on Fig. 13 of [5]

SYMBOL	PROGRAM
○	TULINUS
□	DULMOVITS
◇	MARGASON-LAMAR
△	GIESING
◺	RUBBERT
◺	LOPEZ-SHEN (EVD)
◊	HAVILAND
□	JORDAN
◇	LAMAR (MULTHOPP)
⌂	WIDNALL
◇	BANDLER (ERA)
▽	ROWE
□	CUNNINGHAM
◇	JACOBS-TSAKONAS
◇	LOPEZ (KÜCHEMANN)

Table 4 Identification of Symbols in Fig. 5

where $\tilde{s}_H$ is the transformed chordwise coordinate evaluated at the position of the flap hinge. For a 50% flap the present program gives $C_{L\delta}/C_{L\alpha} = .807$ compared with a value of .818 obtained from (6.1). For a 20% flap the computed value is .526 vs. .550 obtained from (6.1). We should expect slightly lower results for an aspect ratio of 60 so that this result seems reasonable.

The calculation for an aspect ratio of 60 also provided an additional check on $C_{L\alpha}$ in the limit of high aspect ratio. The value obtained was 5.915 which compares closely with a value of 6.080 which one would obtain from the lifting-line theory.

It may also be of some interest to compare the value of $C_{L\alpha}$ given by the present program with that given by Equation (23a) of Chapter VIII of Principles of Naval Architecture [8]. The latter is a simple empirical equation:

$$C_{L\alpha} = \frac{(0.9)\ (2\pi)a}{(\cos\Lambda \sqrt{\frac{a^2}{\cos^4\Lambda} + 4}) + 1.8} \tag{6.2}$$

which, for an aspect ratio $a = 2.8$ and a sweep angle $\Lambda = 15^\circ$ gives a value of 2.997, which is about five percent below the computed value of 3.138. Since (6.2) was developed to provide correlation with experimental results, the lower value of lift slope is not at all unreasonable.

7. DESIGN APPLICATION

The present program was initially developed to provide a rational basis for selecting optimum planforms for an experimental series of flapped rudders [9]. The first two rudders in this series were to have an effective aspect ratio of 2.8 and flap area ratios of 20% and 10%, respectively. These were planned as an extension of an earlier series of experiments on flapped rudders published in 1972 [10].

With such small flaps, minor changes in sweep angle and taper ratio have a large effect on the spanwise distribution of flap chord. The objective is to determine the sweep angle and taper ratio in such a way as to optimise the following parameters:

a) Maximize lift slopes $C_{L\alpha}$ and $C_{L\delta}$;

b) Minimize induced drag;

c) Provide nearly uniform distribution of C_L over span. This requirement is based on a decision to use a constant thickness/chord ratio of 15% over the span. Uniform lift coefficient is then optimum both for delay of cavitation inception and delay of stall.

d) Provide sufficient flap tip chord to permit installation of a hinge.

Calculations were made for five combinations of taper ratio and sweep for the 20% flap rudder and the principal results are given in Table 5. Plots of spanwise distribution of lift-slopes are shown in Fig. 6.

Table 5

Effect of Sweep and Taper on Flapped Rudder Characteristics
effective aspect ratio = 2.8

No.	f	Λ	λ	$C_{L\alpha}$	$C_{L\delta}$	$C_{Di\alpha}$	$C_{Di\delta}$
1	0.2	11^{o}	0.9	3.101	1.670	0.115	0.121
2	"	11^{o}	0.6	3.146	1.802	0.114	0.115
3	"	15^{o}	0.6	3.138	1.775	0.114	0.116
4	"	18^{o}	0.6	3.129	1.738	0.114	0.117
5	"	19.57^{o}	0.5	3.136	1.774	0.114	0.115
6	0.1	15^{o}	0.6	3.138	1.355	0.114	0.119

It is clear from Table 5 that overall lift and drag characteristics are very insensitive to sweep and taper within the fairly limited range permitted due to the small flap. This is, of course, a characteristic of low aspect ratio lifting surfaces, so that this result is not surprising. If one looks closely, one can see the trend of decreasing lift slope and increasing drag with increasing sweep angle.

The effect of taper ratio on spanwise distribution of lift is much more pronounced, as is evident from Fig. 6. Here it is clear that a taper ratio of 0.9 unloads the tip too much, while a taper ratio of 0.5 does the reverse, and that a value of 0.6 seems about right. A change in sweep angle from 11 to 18 degrees has essentially no effect on $C_{L\alpha}$, and a small effect on $C_{L\delta}$.

Rudder No. 2 appears to have the best spanwise distribution of lift as well as maximum lift and minimum drag. However, the tip chord of the flap is extremely small, which would cause difficulties in the model and possibly

in the full-scale hinge design. An increase in sweep angle from 11 to 15 degrees overcomes this problem with very little compromise in performance. Rudder No. 3 was therefore selected for the test program. This has the additional practical advantage of a nearly vertical trailing edge and a constant flap chord.

The constraint on flap chord for the 10% flap area ratio rudder is even more severe. Rudder No. 6 shown in Table 5 and Fig. 6 has the same planform as No. 3, but with a flap area of 10%. Again, we find that $C_{L\delta}$ is a little too low at $z = 0$. Increasing this by a decrease in sweep angle is even more impractical in this case due to the small flap chord. We conclude, therefore, that this planform seems to be nearly optimum for both the 20% and 10% flap rudders.

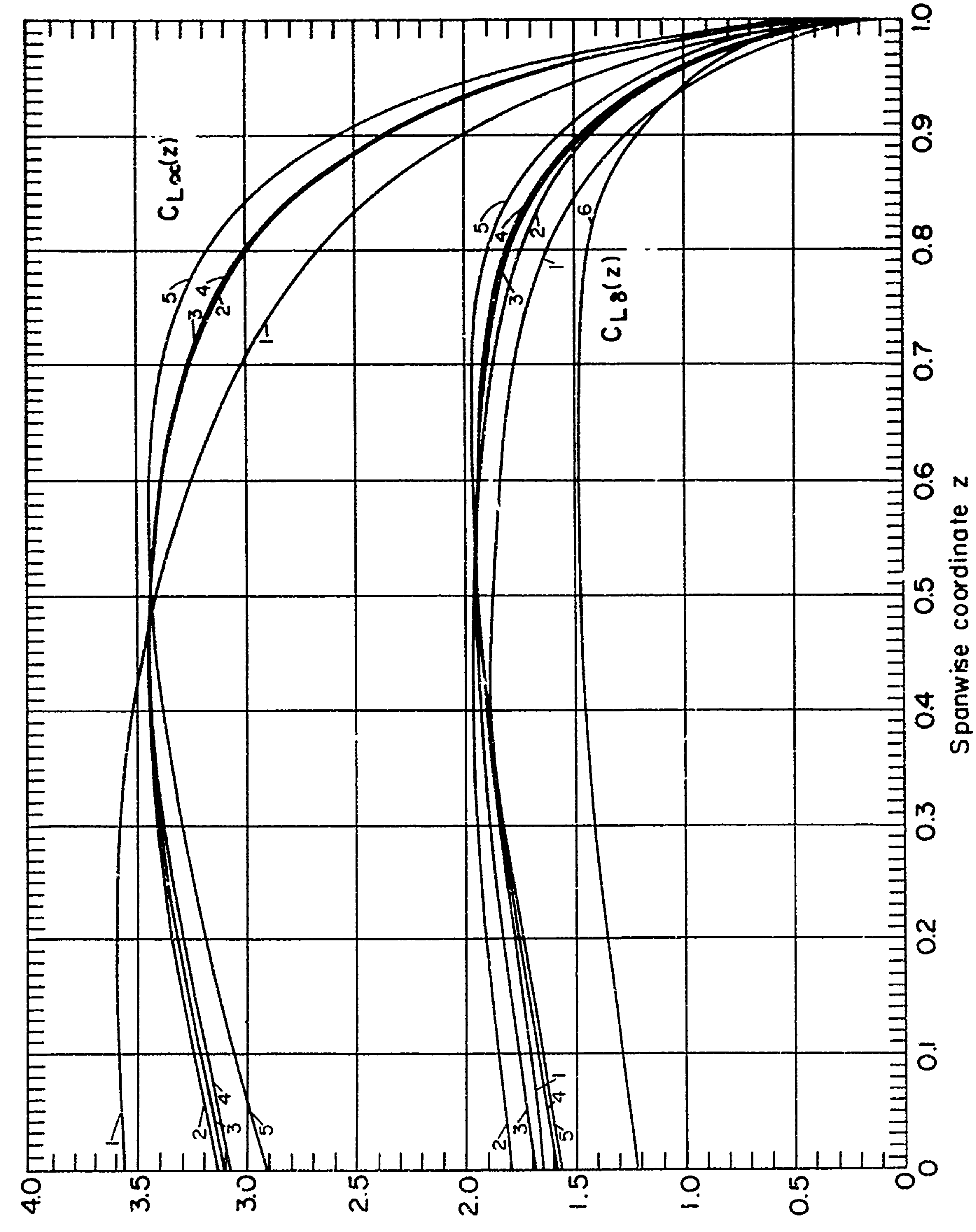

Fig. 6 Spanwise Distribution of Lift due to Angle of Attack and Flap Deflection for Rudder Designs of Table 6

REFERENCES

[1] Falkner, V. M., "The Calculation of Aerodyanmic Loading on Surfaces of Any Shape", *Aerodynamic Research Counsel*, TR R&M, 1973

[2] Kerwin, J. E., "Computer Techniques for Propeller Blade Section Design", *Second Lips Propeller Symposium*, Drunnen, Holland, May, 1973.

[3] Abbott, I. H. and Von Doenhoff, A. E., *Theory of Wing Sections Including a Summary of Airfoil Data*, Dover Publications, Inc., New York, 1959.

[4] Glauert, H., "The Elements of Airfoil and Airscrew Theory", Cambridge University Press, London, 1926.

[5] Langan, T. J. and Wang, H. T., "Evaluation of Lifting Surface Programs for Computing the Pressure Distribution on Planar Foils in Steady Motion", NSRDC 4021, May, 1973.

[6] Watkins, C. E., Woolston, D. S., and Cunningham, H. J., "A Systematic Viernel Function Procedure for Determining Aerodynamic Forces on Oscillating or Steady Finite Wings at Subsonic Speeds", NASA TR R-48, 1959.

[7] Durand, W. F., (Editor in Chief), *Aerodynamic Theory*, Dover Publications, Inc., New York, 1963.

[8] Comstock, J. P. (Editor), *Principles of Naval Architecture*, The Society of Naval Architects and Marine Engineers, New York, 1967.

[9] Kerwin, J. E., Lewis, S. D., and Oppenheim, B. W., "Experiments on Rudders with Small Flaps in Free Stream and Behind a Propeller", M.I.T. Report 74-16, July, 1974.

[10] Kerwin, J. E., Mandel, P., and Lewis, S. D., "An Experimental Study of a Series of Flapped Rudders", *Journal of Ship Research*, December, 1972.

A P P E N D I C E S

APPENDIX 1

Instructions for Preparing Computer Program Input Data

Integer variables must be right-adjusted in their fields - Real variables must contain a decimal somewhere within their field.

A. FIRST CARD

SYMBOL	MODE	FIELD	LIMITATIONS	DESCRIPTION
KDM	Integer	4	1-6	Number of spanwise modes-K Recommended value is 6
LT	Integer	8	3	Number of chordwise modes-L Recommended value is 6
IHF	Integer	12	0,1 or 2	Chordwise precision index I_H Recommended value is 0
IV	Integer	16	0,1 or 2	Spanwise precision index I_V Recommended value is 0
ASR	Real	17-24	*	Geometric aspect ratio, $\frac{1}{2}a$
AF	Real	25-32	$0.1 \leq AF \leq 0.9$	Flap area ratio, f
T	Real	33-40	*	Taper ratio, λ
PP	Real	41-48	*	Sweep angle in degrees, Λ
KOPT	Integer	56	0 or 1	If KOPT=1, the subroutine OPTION will be called and will perform the calculations appearing on the third page of the output

B. SECOND CARD

This card contains the indices of the ten chordwise panels which contain control points, NCP(N),N=1,10. These are integers which are read in ten

*Combinations of these quantities must be so chosen that flap chords are positive for all z.

fields of 8 columns. The recommended values for zero precision number are 3, 8, 13, 18, 23, 28, 33, 38, 42, and 48. However, the intention is that these may be altered for a more advantageous placement relative to the flap hinge if so desired.

C. MULTIPLE RUNS

Upon completion of the calculation, the program returns to the read statement for the first card. A blank card (or more specifically, a zero value for KDM) terminates the run.

APPENDIX 2

Sample Output

The correspondence between the output and the text symbols is as follows:

text	output	text	output
z	Z	$C_{M\alpha}(z) = \frac{x_H^{(\alpha)}(z)}{c(z)} \cdot C_{L\alpha}(z)$	CM-A
$C_{L\alpha}(z)$	CLA	$C_{M\delta}(z) = \frac{x_H^{(\delta)}(z)}{c(z)} \cdot C_{L\delta}(z)$	CM-D
$C_{L\delta}(z)$	CLD	α	ALPHA
$C_{L\alpha}$	CLAR	δ	DELTA
$C_{L\delta}$	CLDR	δ/α	DELTA/ALPHA
$C_{Di\alpha}/C_{L\alpha}^2$	CDIA	$C_L = C_{L\alpha} \cdot \alpha + C_{L\delta} \cdot \delta$	CL
$C_{Di\delta}/C_{L\delta}^2$	CDID	$C_{Di} + C_{DV}$	CD
η^{α}	EFA	$(C_{L\alpha} \cdot C_M \cdot \alpha^2 + C_{L\delta} \cdot C_{L\delta} \cdot \delta^2)/C_L$	CM
η^{δ}	EFD	$(\frac{x_H^{\alpha}}{c} \cdot C_{L\alpha} \cdot \alpha + \frac{x_H^{\delta}}{c} \cdot C_{L\delta} \cdot \delta)/C_L$	XHL/C
$v_{m,n}$	downwash velocities		
c_{KL}^{α}	C-ALPHA		
c_{KL}^{δ}	C-DELTA		
$\frac{x_H^{(\alpha)}(z)}{c(z)}$	XA/LC		
$\frac{x_H^{(\delta)}(z)}{c(z)}$	XD/LC		
$\frac{x_{LE}^{(\alpha)}(z)}{c(z)}$	XALE/LC		
$\frac{x_{LE}^{(\delta)}(z)}{c(z)}$	XDLE/LC		

ASPECT RATIO= 2.80 FLAP AREA=.200 TAPER RATIO=0.60 SWEEP ANGLE=15.000 DEG.
PRECISION INDICES:CHORDWISE =0 SPANWISE=0
NUMBER OF SPANWISE MODES = 6 NUMBER OF CHORDWISE MODES = 6

SPANWISE DISTRIBUTION OF LIFT
Z = SPAN COORDINATE (Z=0 AT THE ROOT,Z =1 AT THE TIP)

Z	CLA	CLD
0.0	3.104	1.693
0.050	3.164	1.717
0.100	3.220	1.753
0.150	3.271	1.789
0.200	3.317	1.824
0.250	3.357	1.856
0.300	3.389	1.884
0.350	3.413	1.907
0.400	3.429	1.923
0.450	3.434	1.933
0.500	3.429	1.937
0.550	3.412	1.935
0.600	3.382	1.929
0.650	3.335	1.916
0.700	3.264	1.894
0.750	3.159	1.854
0.800	3.001	1.783
0.850	2.758	1.661
0.900	2.380	1.456
0.925	2.111	1.304
0.950	1.758	1.100
0.975	1.262	0.803
0.995	0.568	0.368
1.000	0.0	0.0

OVERALL LIFT SLOPE COEFF. PER RADIAN CLAR= 3.138 CLDR= 1.776
INDUCED DRAG COEFF./UNIT LIFT COEFF.**2 CDIA= 0.114 CDID= 0.116
EFFICIENCIES ARE RESPECTIVELY EFA= 0.996 EFD = 0.984

MODE AMPLITUDES C-ALPHA
K DENOTES SPANWISE MODE, L DENOTES CHORDWISE MODE

	K=1	K=2	K=3	K=4	K=5	K=6
L=1	0.38337	0.05644	0.01867	0.01509	0.00131	0.00343
L=2	-0.02663	-0.04391	-0.01702	-0.01471	-0.00742	-0.00348
L=3	0.00410	-0.01519	-0.01336	-0.01182	-0.00436	-0.00760
L=4	0.00493	-0.00349	-0.00635	-0.00591	-0.00315	-0.00154
L=5	0.00344	-0.00022	-0.00254	-0.00274	-0.00737	-0.00124

MODE AMPLITUDES C-DELTA

	K=1	K=2	K=3	K=4	K=5	K=6
L=1	0.03184	0.00299	0.00094	-0.00145	0.00271	-0.00050
L=2	0.12811	0.00303	-0.00524	-0.00001	-0.00589	0.00109
L=3	-0.02836	0.00955	0.00154	0.00312	-0.00029	-0.00027
L=4	0.03670	0.00281	-0.00339	0.00455	-0.00563	0.00244
L=5	0.02933	0.00697	0.00748	0.00011	-0.00147	-0.00109
L=6	0.04199	0.00845	0.00609	0.00140	0.00213	-0.00024

ASPECT RATIO= 2.80 FLAP AREA=.200 TAPER RATIO=0.60 SWEEP ANGLE=15.000 DEG.
PRECISION INDICES:CHORDWISE =0 SPANWISE=0
NUMBER OF SPANWISE MODES = 6 NUMBER OF CHORDWISE MODES = 6

MATRIX OF DOWNWASH VELOCITIES AT ALL CONTROL POINTS
M DENOTES SPANWISE INDEX, N DENOTES CHORDWISE INDEX

DUE TO ALPHA

	N=1	N=2	N=3	N=4	N=5	N=6	N=7	N=8	N=9	N=10
M=1	1.02080	1.01116	1.01427	1.00965	1.00305	0.99899	0.99847	0.99976	1.00008	0.99609
M=2	0.96733	0.96239	0.97996	0.98733	0.99302	0.99241	0.99632	1.00106	1.00412	1.00172
M=3	1.02162	1.00903	1.01750	1.01494	1.00914	1.00314	1.00235	1.00461	1.00584	0.99946
M=4	1.00681	0.99565	1.00701	1.00433	0.99656	0.99097	0.99077	0.99471	0.99770	0.99034
M=5	0.99970	0.97749	0.99438	0.99995	0.99997	0.99954	1.00146	1.00599	1.01031	1.00658
M=6	1.01415	0.99568	1.01201	1.01973	1.00253	0.99502	0.99274	0.99644	1.00129	0.99162
M=7	1.00180	0.97540	1.00181	1.00650	1.00176	0.99539	0.99479	1.00150	1.01019	0.99965
M=8	0.99924	1.00642	1.00358	0.99766	0.99761	1.00075	1.00275	1.00064	0.99525	1.00047

DUE TO DELTA

	N=1	N=2	N=3	N=4	N=5	N=6	N=7	N=8	N=9	N=10
M=1	-0.03657	0.04400	0.02941	-0.00950	-0.02993	-0.00497	0.05994	-0.01547	0.93995	1.03651
M=2	-0.01309	0.09995	-0.04208	-0.12578	-0.06381	0.06318	0.15202	-0.01752	0.87755	1.05137
M=3	-0.06589	0.12095	0.01788	-0.07387	-0.05676	0.03937	0.12188	-0.01365	0.85965	1.07656
M=4	-0.06024	0.12134	0.00771	-0.09038	-0.06954	0.03893	0.13329	-0.01200	0.86414	1.05579
M=5	-0.03746	0.11904	-0.01052	-0.11144	-0.08395	0.04464	0.15288	-0.00392	0.88364	1.05077
M=6	-0.05973	0.12796	0.01428	-0.09099	-0.07694	0.03438	0.14183	0.00933	0.86791	1.04599
M=7	-0.07088	0.12723	0.01998	-0.09446	-0.08946	0.02299	0.13937	0.00422	0.89483	1.04081
M=8	-0.05432	0.12162	0.01434	-0.09399	-0.08150	0.03343	0.13969	-0.00431	0.88647	1.04294

CONTROL POINT COLUMNS ARE LOCATED AT THE DOWNSTREAM BOUNDARIES OF THE FOLLOWING PANELS :

3 8 13 18 23 28 33 38 43 48

ASPECT RATIO= 2.80 FLAP AREA=.200 TAPER RATIO=0.60 SWEEP ANGLE=15.000DEG. PRECISION INDICES:CHORDWISE =0 SPANWISE=0
NUMBER OF SPANWISE MODES = 6 NUMBER OF CHORDWISE MODES = 6

	Z	XA/LC	CM-A	XD/LC	CM-D	XALE/LC	XDLE/LC
	0.0	-0.589	-1.8270	-0.251	-0.4230	0.251	0.589
	0.10	-0.584	-1.8809	-0.247	-0.4333	0.249	0.586
	0.20	-0.582	-1.9321	-0.245	-0.4468	0.244	0.581
	0.30	-0.581	-1.9654	-0.244	-0.4590	0.237	0.575
	0.40	-0.578	-1.9810	-0.242	-0.4652	0.232	0.568
	0.50	-0.572	-1.9613	-0.239	-0.4622	0.228	0.561
	0.60	-0.565	-1.9122	-0.233	-0.4490	0.224	0.557
	0.70	-0.561	-1.8310	-0.226	-0.4238	0.217	0.554
	0.80	-0.561	-1.6821	-0.212	-0.3777	0.204	0.553
	0.90	-0.566	-1.3468	-0.195	-0.2844	0.184	0.555
INTEGRATED		-0.575	-1.8033	-0.234	-0.4156	0.225	0.566

SPANWISE POSITIONS OF THE CENTERS OF PRESSURE ARE : ZA= 0.46 ZD= 0.47

ALPHA	DELTA	DFL/ALPH	CL	CD	L/D	CM	XHL/C
0.0	0.0	******	0.0	0.0085	0.0	0.0	********
0.0	5.0	******	0.1549	0.0117	13.275	-0.03627	-0.2341
0.0	10.0	******	0.3099	0.0212	14.627	-0.07254	-0.2341
0.0	15.0	******	0.4648	0.0370	12.548	-0.10880	-0.2341
0.0	20.0	******	0.6198	0.0592	10.461	-0.14507	-0.2341
0.0	25.0	******	0.7747	0.0878	8.825	-0.18134	-0.2341
5.0	0.0	0.0	0.2738	0.0183	14.961	-0.15737	-0.5747
5.0	2.5	0.5	0.3513	0.0247	14.344	-0.12667	-0.4996
5.0	5.0	1.0	0.4286	0.0326	13.150	-0.11361	-0.4516
5.0	7.5	1.5	0.5063	0.0421	12.014	-0.11010	-0.4183
5.0	10.0	2.0	0.5937	0.0533	10.961	-0.11233	-0.3939
5.0	12.5	2.5	0.6612	0.0660	10.025	-0.11829	-0.3751
10.0	0.0	0.0	0.5477	0.0477	11.478	-0.31474	-0.5747
10.0	5.0	0.5	0.7026	0.0732	9.605	-0.25333	-0.4996
10.0	10.0	1.0	0.8576	0.1049	8.173	-0.22722	-0.4516
10.0	15.0	1.5	1.0125	0.1431	7.078	-0.22320	-0.4183
10.0	20.0	2.0	1.1675	0.1875	6.226	-0.22467	-0.3939
10.0	25.0	2.5	1.3224	0.2383	5.549	-0.23659	-0.3751
15.0	0.0	0.0	0.8215	0.0967	8.492	-0.47211	-0.5747
15.0	7.5	0.5	1.0540	0.1540	6.845	-0.38000	-0.4996
15.0	15.0	1.0	1.2864	0.2255	5.705	-0.34083	-0.4516
15.0	22.5	1.5	1.5188	0.3112	4.880	-0.33030	-0.4183
15.0	30.0	2.0	1.7512	0.4113	4.258	-0.33700	-0.3939
15.0	37.5	2.5	1.9836	0.5256	3.774	-0.35489	-0.3751
20.0	0.0	0.0	1.0954	0.1654	6.624	-0.62948	-0.5747
20.0	10.0	0.5	1.4053	0.2671	5.261	-0.50667	-0.4996
20.0	20.0	1.0	1.7152	0.3942	4.351	-0.45444	-0.4516
20.0	30.0	1.5	2.0250	0.5467	3.704	-0.44040	-0.4183
20.0	40.0	2.0	2.3349	0.7246	3.222	-0.44934	-0.3939

APPENDIX 3

Computer Program Listing and Particulars

Timing Information: 0 precision with 36 modes;

1.081 minutes execution time.

IBM System 370/165

Memory Requirement 100K

```
0001              DIMENSION ZGP(31),ZCP(8),XCP(8,10),XGP(31,70),DWNWSA(8,10),DWNWSD(
                 18,10),V(8,10,6,6),O(8,10),E(6),P(6),CLA(24),CLD(24)
0002              DIMENSION WW(80,37),CA(38),CD(38),ZMP(71),NCP(10),CAA(36),CDD(36)
0003       2      READ(5,1)KOM,LT,IHF,IVER,ASR,AF,T,PP,KOPT
0004       1      FORMAT (4I4,4F8.3,I8)
0005              IF(KOM.EQ.0) STOP
0006              READ(5,4)(NCP(N),N=1,10)
0007       4      FORMAT (10I9)
          C       CALCULATION OF GRID AND CONTROL POINT COORDINATES ****************
0008              AR=2*ASR
0009              W2=0.5*TAN(PP*3.14159/180.0)
0010              CZYN=4.0*AF*(T+1.0)
0011              DENR=2.0*AR*(T+1.0)
0012              FROOT=(CZYN-3.0*(T-1.0))/DENR-W2
0013              SROOT=-((5.0+3.0*T-CZYN)/DENR+W2)
0014              STIP=-((5.0*T+3.0-CZYN)/DENR-W2)
0015              FTIP=(3.0*(T-1.0)+CZYN)/DENR+W2
0016              IF(SROOT.LT.0.0.AND.STIP.LT.0.0.AND.FROOT.GT.0.0.AND.FTIP.GT.0.0)G
                 1O TO 14
0017              WRITE(6,1003)AR,AF,T,PP,IHF,IVER,KOM,LT
0018              WRITE (6,15)
0019      15       FORMAT(///,' ERROR IN THE INPUT DATA: SWEEP ANGLE OR FLAP AREA IS
                 1 TOO BIG OR TAPER RATIO IS TOO SMALL ')
0020              GO TO 2
0021      14      INDX=KOM*(LT-1)
0022              LIT=LT-1
0023              NUMX=LT*KOM
0024              STR=STIP-SROOT
0025              FTR=FTIP-FROOT
0026              RVER=FLOAT(IVER)
0027              RM=14.0+10.0*RVER
0028              LK2=21+5*IVER
0029              LK3=7+5*IVER
0030              LK4=LK3+1
0031              DO 99 I=1,LK3
0032      99      ZGP(I)=2.0*(FLOAT (I)-1.0)/RM
0033              DO 101 I=LK4,LK2
0034     101      ZGP(I)=ZGP(I-1)+2.0/(14.0*RM)
0035              ZCP(1)=1.0/RM
0036              DO 105 K=2,6
0037              FK=FLOAT(K)
0038     105      ZCP(K)=(2.0*FK-1.0+2.0*RVER*(FK-1.0))/RM
0039              ZCP(7)=2.0*(RM/2.0-1.0)/RM+9.0/(14.0*RM)
0040              ZCP(8)=2.0*(RM/2.0-1.0)/RM+19.0/(14.0*RM)
0041              NF=AF*FLOAT(50+IHF*10)+0.1
0042              NS=50+10*IHF-NF
0043              RNS=FLOAT(NS)
0044              RNF=FLOAT(NF)
0045              DO 17 I=1,LK2
0046              XS=ZGP(I)*STR+SROOT
0047              XF=ZGP(I)*FTR+FROOT
0048              DO 16 J=1,NS
0049      16      XGP(I,J)=XS *(FLOAT(NS-J+1)-0.50)/FLOAT(NS)
```

```
      NS1=NS+1
      NT=NS+NF
      DO 17 J=NS1,NT
   17 XGP(I,J)=XF *(FLOAT(J-NS-1)+0.50)/FLOAT(NF)
      DO 20 K=1,8
      XSCP=ZCP(K)*STR+SROOT
      XFCP=ZCP(K)*FTR+FROOT
      DO 20 N=1,10
      IF(NCP(N).GT.NS) GO TO 19
      XCP(K,N)=XSCP*FLOAT(NS-NCP(N))/FLOAT(NS)
      GO TO 20
   19 XCP(K,N)=XFCP*FLOAT(NCP(N)-NS)/FLOAT(NF)
   20 CONTINUE
C     CALCULATION OF INDUCED VELOCITIES ********************************
      DO 1100 KD=1,NUNK
      CA(KD)=0.0
 1100 CB(KD)=0.0
      DO 759 KD=1,KDM
      DO 759 L=1,LT
      DO 759 K=1,8
      DO 759 N=1,10
  759 V(K,N,KD,L)=0.0
      LWS=LK2-1
      DO 720 I=1,LWS
      ZMS=0.5*(ZGP(I+1)+ZGP(I))
      XS=ZMS*STR+SROOT
      XF=ZMS*FTR+FROOT
      CGPT=ZMS*(FTR-STR)+FROOT-SROOT
      ZWIG=ARCOS(-ZMS)
      DO 500 KD=1,KDM
  500 E(KD)=SIN((2.0*FLOAT(KD)-1.0)*ZWIG)
      DO 720 J=1,NT
      FJ=FLOAT(J)
      DO 721 K=1,8
      DO 721 N=1,10
      ICOMM=I
      JCOMM=J
      KCOMM=K
      NCOMM=N
  721 Q(K,N)=HSVEL(XGP(I,J),ZGP(I),XGP(I+1,J),ZGP(I+1),XCP(K,N),ZCP(K))
      IF (J.GT.NS) GO TO 600
      SS2=-XS*FJ/(RNS*CGPT)
      SS1=-XS*(FJ-1.0)/(RNS*CGPT)
      SSW2=ARCOS(1.0-2.0*SS2)
      SSW1=ARCOS(1.0-2.0*SS1)
      P(1)=SSW2+SIN(SSW2)-SSW1-SIN(SSW1)
      P(2)=SSW2-0.5*SIN(2.0*SSW2)-SSW1+0.5*SIN(2.0*SSW1)
      IF (LT.LE.3) GO TO 710
      DO 609 L=3,LIT
      FL=FLOAT(L)
  609 P(L)=(SIN((FL-2.0)*SSW2)-SIN((FL-2.0)*SSW1))/(FL-2.0)+(SIN(FL*SSW
     11)-SIN(FL*SSW2))/FL
      GO TO 710
```

```
 600  FJOT=FLOAT(J-NS)
      SF2=(XF*FJOT-RNF*XS)/(RNF*CGPT)
      SF1=(XF*(FJOT-1.0)-RNF*XS)/(RNF*CGPT)
      SFW2=ARCOS(1.0-2.0*SF2)
      SFW1=ARCOS(1.0-2.0*SF1)
      P(1)=SFW2+SIN(SFW2)-SFW1-SIN(SFW1)
      P(2)=SFW2-0.5*SIN(2.0*SFW2)-SFW1+0.5*SIN(2.0*SFW1)
      IF (LT.LE.3) GO TO 700
      DO 704 L=3,LT
      FL=FLOAT(L)
 704  P(L)=(SIN((FL-2.0)*SFW2)-SIN((FL-2.0)*SFW1))/(FL-2.0)+(SIN(FL*SFW1
     1)-SIN(FL*SFW2))/FL
 700  T2=FJOT/RNF
      T1=(FJOT-1.0)/RNF
      TW2=ARCOS(1.0-2.0*T2)
      TW1=ARCOS(1.0-2.0*T1)
      LIT=LT
      P(LT)=TW2+SIN(TW2)-TW1-SIN(TW1)
 710  DO 760 K=1,8
      DO 760 N=1,10
      DO 760 KD=1,KDM
      DO 760 L=1,LIT
 760  V(K,N,KD,L)=V(K,N,KD,L)+Q(K,N)*F(KD)*P(L)
 720  CONTINUE
C       CALCULATION OF BOUNDARY CONDITIONS    **************************
      DO 801 K=1,8
      DO 801 N=1,10
      DWNWSA(K,N)=0.0
 801  DWNWSD(K,N)=0.0
      LT5=LT-1
      NUNK=KDM*(LT-1)
      MUNK=NUNK+1
      DO 805 N=1,10
      DO 805 K=1,8
      IV=(N-1)*8+K
      DO 800 L=1,LT5
      DO 800 KD=1,KDM
      IH=(L-1)*KDM+KD
 800  WW(IV,IH)=V(K,N,KD,L)
 805  WW(IV,MUNK)=1.0
      CALL PTLSQ (WW,CA,80,NUNK,KERROR)
      DO 803 N=1,10
      DO 803 K=1,8
      DO 803 KD=1,KDM
      DO 803 L=1,LT5
      IS=(L-1)*KDM+KD
 803  DWNWSA(K,N)=V(K,N,KD,L)*CA(IS)+DWNWSA(K,N)
      NUNK=KDM*LT
      MUNK=NUNK+1
      DO 815 N=1,10
      DO 815 K=1,8
      IV=(N-1)*8+K
      DO 810 L=1,LT
```

```
      DO 810 KD=1,KDM
      IH=(L-1)*KDM+KD
  810 WW(IV,IH)=V(K,N,KD,L)
      WW(IV,MUNK)=1.0
      IF(XCP(K,N).LT.0.0) WW(IV,MUNK)=0.0
  815 CONTINUE
      CALL PTLSQ(WW,CC,RO,NUNK,KERROR)
      DO 804 N=1,10
      DO 804 K=1,8
      DO 804 KD=1,KDM
      DO 804 L=1,LT
      IS=(L-1)*KDM+KD
  804 DWNWSD(K,N)=V(K,N,KD,L)*CO(IS)+DWNWSD(K,N)
C       CALCULATIONS OF FORCES    ****************************************
      CLAG=(3.14159**3)*AR*(CA(1)+CA(1+KDM))
      CLDG=(3.14159**3)*AR*(CD(1)+CD(1+KDM)+CD(1+INDX))
      SM1=0.0
      SM2=0.0
      ZMP(1)=0.0
      DO 910 I=2,22
      IF (I.LE.19) ZMP(I)=ZMP(I-1)+0.05
      IF (I.GT.19) ZMP(I)=ZMP(I-1)+0.025
  910 CONTINUE
      ZMP(23)=0.995
      ZMP(24)=1.0
      CLA(24)=0.0
      CLD(24)=0.0
      DO 911 I=1,23
      SUM1=0.0
      SUM2=0.0
      CGPT=ZMP(I)*(FTR-STR)+FRCCT-SROOT
      ZWIG=ARCOS(-ZMP(I))
      DO 912 KD=1,KDM
      FD=FLOAT(KD)
      E(KD)=SIN((2.0*FD-1.0)*ZWIG)
      SUM1=SUM1+E(KD)*(CA(KD)+CA(KD+KDM))*2.0/CGPT
  912 SUM2=SUM2+E(KD)*(CD(KD)+CD(KD+KDM)+CD(KD+INDX))*2.0/CGPT
      CLA(I)=39.47842*SUM1
  911 CLD(I)=39.47842*SUM2
      AA1=CA(1)+CA(1+KDM)
      AA2=CD(1)+CD(1+KDM)+CD(1+INDX)
      DO 913 KD=2,KDM
      FK=FLOAT(KD)
      SM1=SM1+(2.0*FK-1.0)*((CA(KD)+CA(KD+KDM))/AA1)**2
  913 SM2=SM2+(2.0*FK-1.0)*((CD(KD)+CD(KD+KDM)+CD(KD+INDX))/AA2)**2
      CDIA=(1.0+SM1)/(3.14159*AR)
      CDID=(1.0+SM2)/(3.14159*AR)
      EFA=1.0/(1.0+SM1)
      EFD=1.0/(1.0+SM2)
      KDML=KDM*LT
      DO 915 N=1,KDML
      CAA(N)=CA(N)*9.86958
  915 CDD(N)=CD(N)*9.86958
```

```
0204              WRITE(6,1003)AR,AF,T,PP,IHF,IVER,KDM,LT
0205        1003 FORMAT('1',5X,13HASPECT RATIO=F5.2,2X,10HFLAP AREA=F4.3,2X,12HTAPE
               1R RATIO=F4.2,2X,12HSWEEP ANGLE=F6.3,3X,4HDEG.,/,6X,29HPRECISION IN
               2DICES:CHORDWISE =I1,2X,9HSPANWISE=I1,/,6X,'NUMBER OF SPANWISE MO
               3DES =',I2,5X,'NUMBER OF CHORDWISE MODES =',I2,//)
0206              WRITE (6,948)
0207         948 FORMAT (10X,29HSPANWISE DISTRIBUTION OF LIFT,/,10X,'Z = SPAN COORD
               1INATE  (Z=0 AT THE ROOT,Z =1 AT THE TIP)',///)
0208              WRITE(6,946)
0209         946  FORMAT(16X,1HZ,14X,3HCLA,12X,3HCLD)
0210              DO 950 I=1,24
0211         950  WRITE(6,949)ZMP(I),CLA(I),CLD(I)
0212         949  FORMAT (10X,3(F10.3,5X))
0213              WRITE(6,991)CLAG,CLDG
0214         991  FORMAT(//,9X,'OVERALL LIFT SLOPE COEFF. PER RADIAN    CLAR=',F8.3,
               16X,'CLDR=',F8.3)
0215              WRITE(6,1000)CDIA,CDID
0216        1000 FORMAT(9X,'INDUCED DRAG COEFF./UNIT LIFT COEFF.**2 CDIA=',F8.3,6X,
               1'CDID=',F8.3)
0217              WRITE(6,961)EFA,EFD
0218         961  FORMAT(9X,29HEFFICIENCIES ARE RESPECTIVELY,12X,4HEFA=F8.3,6X,5HEFD
               1 =F8.3)
0219              WRITE(6,955)
0220         955  FORMAT (/,30X,'MODE AMPLITUDES C-ALPHA')
0221              WRITE(6,1002)
0222        1002  FORMAT(9X,50HK DENOTES SPANWISE MODE,  L DENOTES CHORDWISE MODE)
0223              WRITE(6,1001)
0224        1001 FORMAT (18X,3HK=1,9X,3HK=2,9X,3HK=3,9X,3HK=4,9X,3HK=5,9X,3HK=6)
0225              DO 957 L=1,LT5
0226              KW=(L-1)*KDM+1
0227              KWMAX=KW+KDM-1
0228         958  FORMAT (8X,2HL=,I1,1X,10F12.5)
0229          957 WRITE(6,958)L,(CAA(N),N=KW,KWMAX)
0230              WRITE(6,959)
0231         959  FORMAT (/,30X,'MODE AMPLITUDES C-DELTA')
0232              WRITE(6,1001)
0233              DO 960 L=1,LT
0234              KW=(L-1)*KDM+1
0235              KWMAX=KW+KDM-1
0236          960 WRITE(6,958)L,(CDD(N),N=KW,KWMAX)
0237              WRITE(6,1003) AR,AF,T,PP,IHF,IVER,KDM,LT
0238              WRITE (6,981)
0239         981  FORMAT (///,20X,'MATRIX OF DOWNWASH VELOCITIES AT ALL CONTROL POIN
               1TS',/,20X,'M DENOTES SPANWISE INDEX, N DENOTES CHORDWISE INDEX',/,
               230X,'DUE TO ALPHA          ',/,18X,'N=1',9X,'N=2',9X,'N=3',9X,'N=4
               3',9X,'N=5',9X,'N=6',9X,'N=7',9X,'N=8',9X,'N=9',9X,'N=10')
0240              DO 982 K=1,8
0241         982  WRITE(6,983)K,(DWNWSA(K,N),N=1,10)
0242         983  FORMAT (8X,'M=',I1,1X,10F12.5)
0243              WRITE(6,984)
0244         984  FORMAT (/,30X,'DUE TO DELTA',/,18X,'N=1',9X,'N=2',9X,'N=3',9X,'N=4
               1',9X,'N=5',9X,'N=6',9X,'N=7',9X,'N=8',9X,'N=9',9X,'N=10')
0245              DO  985 K=1,8
```

```
0246          985  WRITE (6,983)K,(DWNWSP(K,N),N=1,10)
0247               WRITE(6,986) (NCP(N),N=1,10)
0248          986  FORMAT (/////,10X,'CONTROL POINT COLUMNS ARE LOCATED AT THE DOWNST
                  1REAM BOUNDARIES OF THE FOLLOWING PANELS :',/,13X,10I10,///)
0249               IF(KOPT.EQ.1) CALL OPTION (CA,CD,KOM,LT,IHF,IVER,AR,AF,T,PP,SROOT,
                  1STIP,FROOT,FTIP)
0250               GO TO 2
0251               END
```

```
              SUBROUTINE PTLSQ (A,R,NEQ,NUN,KERROR)
              DIMENSION A(80,37),R(36),B(1444)
              MUN=NUN+1
              DO 1 M=1,NUN
              DO 1 N=1,NUN
              L=N+(M-1)*NUN
              B(L)=0.0
              DO 1 J=1,NEQ
      1       B(L)=B(L)+A(J,M)*A(J,N)
              DO 2 M=1,NUN
              R(M)=0.0
              DO 2 N=1,NEQ
      2       R(M)=R(M)+A(N,MUN)*A(N,M)
              CALL SIMQ (B,R,NUN,KERROR)
              RETURN
              END
```

```
FORTRAN IV G1  RELEASE 2.0          SIMQ          DATE = 74226          18/06/24          PAGE 0001

      SUBROUTINE SIMQ(A,B,N,KS)                                         SIMQ 490
      DIMENSION A(1),B(1)                                               SIMQ 500
      TOL=0.0                                                           SIMQ 540
      KS=0                                                              SIMQ 550
      JJ=-N                                                             SIMQ 560
      DO 65 J=1,N                                                       SIMQ 570
      JY=J+1                                                            SIMQ 580
      JJ=JJ+N+1                                                         SIMQ 590
      BIGA=0                                                            SIMQ 600
      IT=JJ-J                                                           SIMQ 610
      DO 30 I=J,N                                                       SIMQ 620
      IJ=IT+I                                                           SIMQ 660
      IF(ABS(BIGA)-ABS(A(IJ)))20,30,30
   20 BIGA=A(IJ)                                                        SIMQ 680
      IMAX=I                                                            SIMQ 690
   30 CONTINUE                                                          SIMQ 700
      IF(ABS(BIGA)-TOL)35,35,40
   35 KS=1                                                              SIMQ 750
      RETURN                                                            SIMQ 760
   40 I1=J+N*(J-2)                                                      SIMQ 800
      IT=IMAX-J                                                         SIMQ 810
      DO 50 K=J,N                                                       SIMQ 820
      I1=I1+N                                                           SIMQ 830
      I2=I1+IT                                                          SIMQ 840
      SAVE=A(I1)                                                        SIMQ 850
      A(I1)=A(I2)                                                       SIMQ 860
      A(I2)=SAVE                                                        SIMQ 870
   50 A(I1)=A(I1)/BIGA                                                  SIMQ 910
      SAVE=B(IMAX)                                                      SIMQ 920
      B(IMAX)=B(J)                                                      SIMQ 930
      B(J)=SAVE/BIGA                                                    SIMQ 940
      IF(J-N) 55,70,55                                                  SIMQ 980
   55 IQS=N*(J-1)                                                       SIMQ 990
      DO 65 IX=JY,N                                                     SIMQ1000
      IXJ=IQS+IX                                                        SIMQ1010
      IT=J-IX                                                           SIMQ1020
      DO 60 JX=JY,N                                                     SIMQ1030
      IXJX=N*(JX-1)+IX                                                  SIMQ1040
      JJX=IXJX+IT                                                       SIMQ1050
   60 A(IXJX)=A(IXJX)-(A(IXJ)*A(JJX))                                   SIMQ1060
   65 B(IX)=B(IX)-(B(J)*A(IXJ))                                         SIMQ1070
   70 NY=N-1                                                            SIMQ1110
      IT=N*N                                                            SIMQ1120
      DO 80 J=1,NY                                                      SIMQ1130
      IA=IT-J                                                           SIMQ1140
      IB=N-J                                                            SIMQ1150
      IC=N                                                              SIMQ1160
      DO 80 K=1,J                                                       SIMQ1170
      B(IB)=B(IB)-A(IA)*B(IC)                                           SIMQ1180
      IA=IA-N                                                           SIMQ1190
   80 IC=IC-1                                                           SIMQ1200
      RETURN                                                            SIMQ1210
      END                                                               SIMQ1220
```

```
      FUNCTION HSVEL(X1,Z1,X2,Z2,X,Z)
      HSVEL=0.0
      XA=X1
      ZA=Z1
      XB=X2
      ZB=Z2
      DO 1 N=1,2
      T=(XB-XA)/(ZB-ZA)
      A=1.0+T**2
      E=X-XA+T*ZA
      B=-2.0*(E*T+Z)
      C=E**2+Z**2
      D=E-T*Z
      RAT=1.0
      ZC=ZA
      XC=XA
      DO 2 M=1,2
      HSVEL=HSVEL+RAT*((X-XC)/SQRT((X-XC)**2+(Z-ZC)**2)+1.0)/(Z-ZC)
      IF(ABS(D).GT.0.002) GO TO 3
      IF(N.NE.1.OR.Z.LT.Z1.OR.Z.GT.Z2) GO TO 4
      HSVEL=HSVEL+SQRT(A)*(1.0/D-4.0*D/(2.0*A*ZC+B)**2)
      GO TO 4
    3 HSVEL=HSVEL-RAT*0.5*(2.0*A*ZC+B)/(D*SQRT(A*ZC**2+B*ZC+C))
    4 RAT=-1.0
      XC=XB
    2 ZC=ZB
      XA=X2
      ZA=-Z2
      XB=X1
    1 ZB=-Z1
      RETURN
      END
```

```
0001           SUBROUTINE OPTION(CA,CD,KOM,LT,IHF,IVFR,AR,AF,T,PP,SROOT,STIP,FROO
              1T,FTIP)
0002            DIMENSION CA(30),CD(36),CHM(6),E(6),Z(12),P(6),SIMPSN(11)
0003           DATA SIMPSN/0.33333,1.33333,0.66667,1.33333,0.66667,1.33333,0.6666
              17,1.33333,0.6,1.5085,0.0/
0004           DATA KI/5/,KO/6/
0005           WRITE (KO,1003)AR,AF,T,PP,IHF,IVFR,KOM,LT
0006      1003 FORMAT('1',5X,13HASPECT RATIO=F5.2,2X,10HFLAP AREA=F4.3,2X,12HTAPE
              1R RATIO=F4.2,2X,12HSWEEP ANGLE=F6.3,4HDEG.,2X,20HPRECISION INDICES
              2:CHORDWISE =I1I,2X,9HSPANWISE=I1I,/,6X,'NUMBER OF SPANWISE MODES =
              3',I2,5X,'NUMBER OF CHORDWISE MODES =',I2,//)
0007           CCNT=0.0166
0008           CTM=(FTIP-STIP+FROOT-SROOT)*0.5
0009           XTM=(FROOT+FTIP)*0.5/CTM
0010           INDX=KOM*(LT-1)
0011           WRITE(6,1546)
0012      1546 FORMAT(//,22X,'Z',8X,'XA/LC',8X,'CM-A',8X,'XD/LC',8X,'CM-D',5X,'XA
              1LE/LC',5X,'XDLE/LC',/)
0013           AA1=CA(1)+CA(1+KOM)
0014           AA2=CD(1)+CD(1+KOM)+CD(1+INDX)
0015           CLAG=(3.14159**3)*AR*AA1
0016           CLDG=(3.14159**3)*AR*AA2
0017           CMINA=0.0
0018           CMIND=0.0
0019           ZCPA=0.0
0020           ZCPD=0.0
0021           DO 1515 IR=1,10
0022           CLA=0.0
0023           CLD=0.0
0024           I=IR-1
0025           ZI=FLOAT(I)
0026           Z(IR)=ZI/10.0
0027           XT=Z(IR)*(FTIP-FROOT)+FROOT
0028           XL=Z(IR)*(STIP-SROOT)+SROOT
0029           CT=XT-XL
0030           PPC=XT/CT
0031           ZWIG=ARCOS(-Z(IR))
0032           DO 1520 KD=1,KOM
0033           RD=FLOAT(KD)
0034           E(KD)=SIN((2.0*RD-1.0)*ZWIG)
0035           CLA=CLA+E(KD)*(CA(KD)+CA(KD+KOM))*78.9568/CT
0036      1520 CLD=CLD+E(KD)*(CD(KD)+CD(KD+KOM)+CD(KD+INDX))*78.9568/CT
0037           LW8=LT-1
0038           ZCPA=ZCPA+CLA*Z(IR)/(10.0*CLAG)*SIMPSN(IR)
0039           ZCPD=ZCPD+CLD*Z(IR)/(10.0*CLDG)*SIMPSN(IR)
0040           P(1)=3.14159
0041           P(2)=3.14159
0042           DO 1522 L=3,LW8
0043      1522 P(L)=0.0
0044           P(LT)=3.14159
0045           CHM(1)=3.14159*(CT+4.0*XL)/4.0
0046           CHM(2)=3.14159*(CT+2.0*XL)/2.0
0047           CHM(3)=-3.14159*CT/4.0
```

```
      DO 1525 L=4,LW8
 1525 CMM(L)=0.0
      CMM(LT)=3.14159*XT/4.0
      CMAL=0.0
      CMDL=0.0
      CHA=0.0
      CHD=0.0
      DO 1540 KD=1,KDM
      CMAK=0.0
      CMDK=0.0
      CHAK=0.0
      CHDK=0.0
      DO 1530 L=1,LW8
      MM=KD+KDM*(L-1)
      CHAK=CHAK+CA(MM)*P(L)
 1530 CMAK=CMAK+CMM(L)*CA(MM)
      DO 1535 L=1,LT
      MM=KD+KDM*(L-1)
      CHDK=CHDK+CD(MM)*P(L)
 1535 CMDK=CMDK+CMM(L)*CD(MM)
      CMAL=F(KD)*CMAK+CMAL
      CMDL=F(KD)*CMDK+CMDL
      CHA=F(KD)*CHAK+CHA
 1540 CHD=E(KD)*CHDK+CHD
      XAL=CMAL/(CHA*CT)
      XDL=CMDL/(CHD*CT)
      XLFA=1.0-(PRC-XAL)
      XLFD=1.0-(PRC-XDL)
      CMAZ=XAL*CLA
      CMDZ=XDL*CLD
      WRITE(KO,1550)Z(IP),XAL,CMAZ,XDL,CMDZ,XLFA,XLFD
 1550 FORMAT(20X,F5.2,2(5X,F7.3,4X,F8.4),2(5X,F7.3))
      CMINA=CMINA+CMAZ*CT*SIMPSN(IR)
      CMIND=CMIND+CMDZ*CT*SIMPSN(IR)
 1515 CONTINUE
      SA=CMINA/(CLAG*CTM*10.0)
      SD=CMIND/(CLDG*CTM*10.0)
      CMINA=CMINA/(CTM*10.0)
      CMIND=CMIND/(CTM*10.0)
      XLEAM=1.0-(XTM-SA)
      XLEDM=1.0-(XTM-SD)
      WRITE(KO,1551)SA,CMINA,SD,CMIND,XLEAM,XLEDM
 1551 FORMAT(/,4X,'INTEGRATED',17X,F6.3,5X,F7.4,6X,F6.3,5X,F7.4,2(6X,F6.
     13),/)
      WRITE(KO,1600) ZCPA,ZCPD
 1600 FORMAT(1X,'SPANWISE POSITIONS OF THE CENTERS OF PRESSURE ARE : ZA=
     1',F8.2,5X,'ZD=',F8.2)
      WRITE(KO,1705)
 1705 FORMAT(/,11X,'ALPHA',8X,'DELTA',6X,'DEL/ALPH',9X,'CL',12X,'CD',12X
     1,'L/D',9X,'CM',10X,'XHL/C',/)
      DO 1650 KAL=1,21,5
      DO 1650 KRA=1,26,5
      KALA=KAL-1
```

```
FORTRAN IV G1  RELEASE 2.0           OPTION           DATE = 74276        18/06/24              PAGE 0003

 0098                    KR=KRA-1
 0099                    IF(KALA)1500,1500,1505
 0100               1500 IF(KR)1501,1501,1502
 0101               1501 ALA=0.0
 0102                    DEL=0.0
 0103                    DIV=99999.9
 0104                    GO TO 1510
 0105               1502 ALA=0.0
 0106                    DEL=FLOAT(KR)
 0107                    DIV=99999.9
 0108                    GO TO 1510
 0109               1505 ALA=FLOAT(KALA)
 0110                    R=FLOAT(KR)
 0111                    DEL=ALA*R/10.0
 0112                    DIV=DEL/ALA
 0113               1510 ALPH=ALA/57.296
 0114                    DELT=DEL/57.296
 0115                    AA=AA1*ALPH+AA2*DELT
 0116                    CLALF=CLAG*ALPH
 0117                    CLDEL=CLDG*DELT
 0118                    CL=CLALF+CLDEL
 0119                    SM=0.0
 0120                    IF(AA)1512,1516,1512
 0121               1512 DO 1514 KD=2,KDM
 0122                    RKD=FLOAT(KD)
 0123                    K1=KD+KDM
 0124                    K2=KD+INDX
 0125              1514  SM=SM+(2.0*RKD-1.0)*(((CA(KD)+CA(K1))*ALPH+(CD(KD)+CD(K1)+CD(K2))*
                        1DELT)/AA)**2
 0126                    CR=(CL**2)*(1.0+SM)/(3.14159*AR)+0.C095+CCNT*CL**2
 0127                    GO TO 1517
 0128               1516 CR=C.CC95+CCNT*CL**2
 0129               1517 CLD=CL/CR
 0130                    IF(CL.EQ.0.0)XPC=99999.9
 0131                    IF(CL.EQ.0.0)CM=0.0
 0132                    IF(CL.EQ.0.0) GO TO 1709
 0133                    CM=(CMINA*CLALF*ALPH+CMIND*CLDEL*DELT)/CL
 0134                    XPC=(SA*CLALF+SD*CLDEL)/CL
 0135               1709 WRITE(6 ,1710)ALA,DEL,DIV,CL,CR,CLD,CM,XPC
 0136               1710 FORMAT(9X,F6.1,7X,F6.1,9X,F6.1,7X,F8.4,6X,F8.4,5X,F8.3,6X,F8.5,5X,
                        1F8.4)
 0137               1650 CONTINUE
 0138                    RETURN
 0139                    END
```

APPENDIX 4

Positioning of Control Points Within Their Own Elements

Control points should be located at a point within the element where the effects of the velocities induced by all four boundaries of the element cancel. This is essential in order for the discrete system to converge to the Cauchy-Principal Value of the corresponding continuous singular integral. For a rectangular element this will be, of course, at the centroid of the element.

With the present vortex scheme the elements may be both swept and tapered, so that a question arises as to whether the placement of the control point is critical. A detailed calculation was therefore made for an extreme element with geometric characteristics as shown in Fig. 7.

The velocity induced by the four line vortex elements was computed at finely spaced intervals throughout the interior of the element. In this case, the null point, 0, was found to be displaced from the mid-chord/mid-span point, M, by the amount shown in Fig. 7. This deviation, as well as the velocity at M is extremely small.

In order to obtain an estimate of the error introduced by locating control points at M rather than at 0 in the complete lifting surface program a test run was made with all control points displaced by two percent of their panel chords. This resulted in a change of 0.92% in predicted lift slope. Since this displacement was far in excess of the value shown in Fig. 7, it can be concluded that the error introduced by locating control points at the mid-chord /mid-span position of an element is negligible.

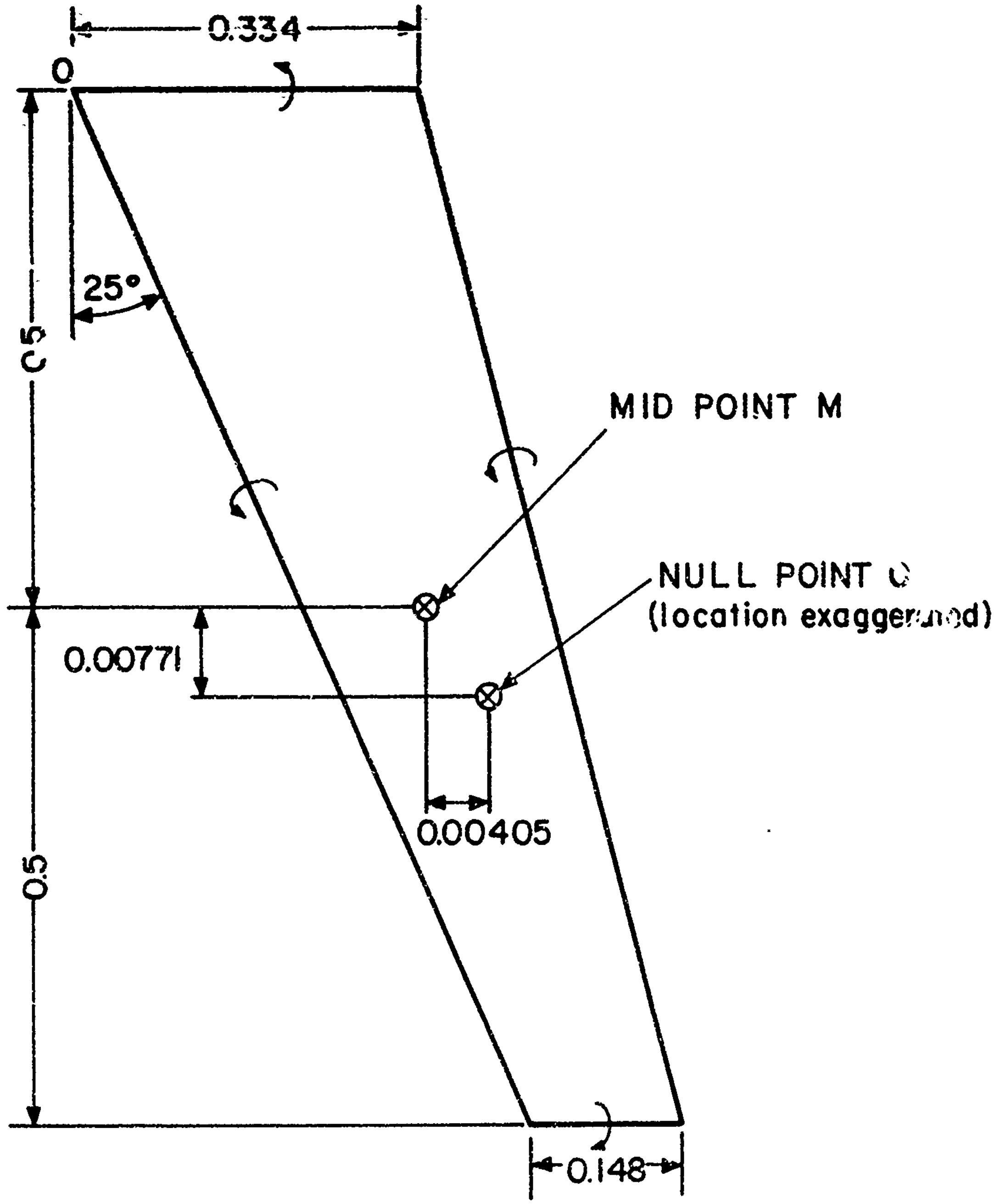

Fig. 7 The Element Used for Estimation of the Error Caused by Control Point Position Deviations